

# Decomposing Epistemic Uncertainty for Causal Decision Making

Md Musfiqur Rahman<sup>\*,1</sup> Ziwei Jiang<sup>\*,2</sup> Hilaf Hasson<sup>3</sup> Murat Kocaoglu<sup>2</sup>

<sup>1</sup>Electrical and Computer Engineering, Purdue University

<sup>2</sup>Computer Science, Johns Hopkins University

<sup>3</sup>Intuit AI Research

`rahman89@purdue.edu, zjiang85@jh.edu, hilaf_hasson@intuit.com, mkocaoglu@jhu.edu`

February 2, 2026

## Abstract

Causal inference from observational data provides strong evidence for the best action in decision-making without performing expensive randomized trials. The effect of an action is usually not identifiable under unobserved confounding, even with an infinite amount of data. Recent work uses neural networks to obtain practical bounds to such causal effects, which is often an intractable problem. However, these approaches may overfit to the dataset and be overconfident in their causal effect estimates. Moreover, there is currently no systematic approach to disentangle how much of the width of causal effect bounds is due to fundamental non-identifiability versus how much is due to finite-sample limitations. We propose a novel framework to address this problem by considering a confidence set around the empirical observational distribution and obtaining the intersection of causal effect bounds for all distributions in this confidence set. This allows us to distinguish the part of the interval that can be reduced by collecting more samples, which we call sample uncertainty, from the part that can only be reduced by observing more variables, such as latent confounders or instrumental variables, but not with more data, which we call nonID uncertainty. The upper and lower bounds to this intersection are obtained by solving min-max and max-min problems with neural causal models by searching over all distributions that the dataset might have been sampled from, and all SCMs that entail the corresponding distribution. We demonstrate via extensive experiments on synthetic and real-world datasets that our algorithm can determine when collecting more samples will not help determine the best action. This can guide practitioners to collect more variables or lean towards a randomized study for best action identification.

## 1 Introduction

Causal decision-making aims to identify the best action relative to an objective function. For example, *which drug maximizes the life expectancy of an average patient? Which candidate government policy should be enacted to reduce unemployment more?* Since actions affect the system relative to its observational state, answering such questions requires causal models. Pearl’s structural causal modeling (SCM) framework provides us with a systematic set of complete algorithmic principles to identify the effect of actions from observational data through the do-operator and do-calculus, under well-defined assumptions (Pearl, 1995; Tian, 2002; Huang and Valdora, 2006; Shpitser and Pearl, 2008), e.g., interventional distribution  $p(y|do(x)) = \theta(p(\mathbf{v}))$  for some function  $\theta$  and observational distribution  $p(\mathbf{v})$ . When the interventional distribution or the causal effect cannot be determined uniquely, the framework can be used to obtain bounds on causal effects (Zhang and Bareinboim, 2021; Hu et al., 2021; Li and Pearl, 2022; Hu et al., 2021).

Identifying causal effects allows us to make decisions about different actions. For example, we wish to know if enforcing a policy  $X = x$  is beneficial at the population level:  $P(y|do(x)) > P(y)$  with the causal effect of  $X = x$  on  $Y = y$  (Jung et al., 2022; Eva and Stern, 2019). Similarly, we can choose the best action

---

<sup>\*</sup>Equal contribution.

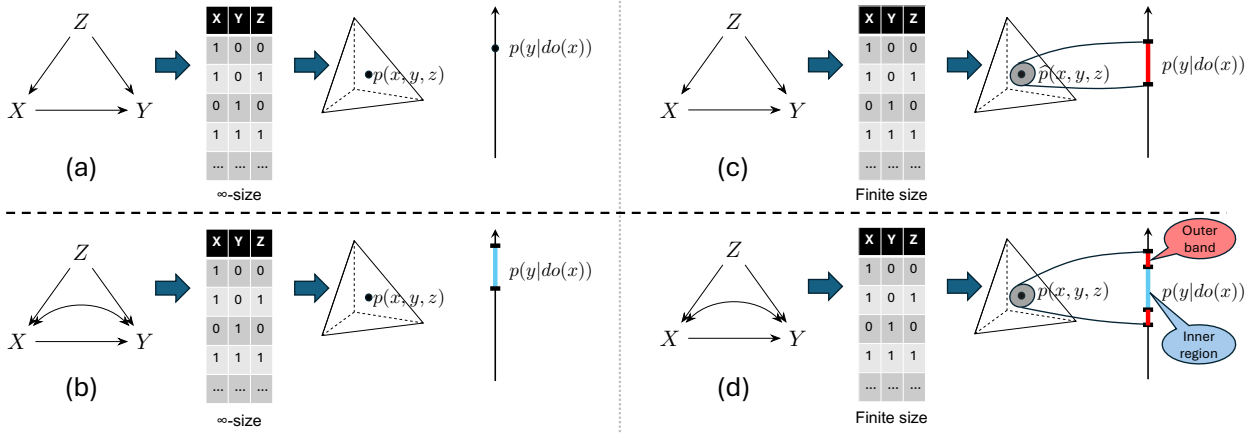


Figure 1: Left: The case of infinite observational data. An identifiable causal effect can be estimated pointwise as in (a). Otherwise, we obtain bounds as in (b). Right: Given finite samples, we cannot pointwise estimate since the true distribution lies in a continuum of a confidence set. We can only obtain an interval as in (c). When the effect is not identifiable, we obtain a larger bound as in (d). Our goal is to analyze which part of this interval is due to non-identifiability and cannot be reduced by collecting more samples.

that maximizes reward by comparing  $P(y|do(x_1))$  and  $P(y|do(x_0))$ . However, a causal effect is not always identifiable; that is, when an observational distribution is compatible with SCMs that induce different values of the causal effect. In practice, usually we do not have access to the observational distribution, but the data sampled from it. So the set of possible observational distributions that correspond to the data introduces additional uncertainty for the causal effect estimation. Fortunately, point estimation of causal effect is not always necessary for causal decision-making (Fernández-Loría and Provost, 2022).

If the utility of two actions are sufficiently different, partial identification of the causal effects, i.e., deriving upper and lower bounds to them, might be sufficient to determine the better action; for example, if the *lower bound* to the utility of Action 1 is greater than the *upper bound* to the utility of all other actions, we can still decide Action 1 is more desirable than the others. Also note that if the bounds are tight, then the slightest overlap of two causal effect bounds should lead any causal decision-making algorithm to say "*I do not know, yet*" since either action may be optimal. Especially for safety-critical applications, *knowing when we do not know* is crucial. It is then clear that obtaining tight causal effect bounds from observational data, and doing this efficiently in practice, is necessary for effective causal decision-making. Surprisingly, a practical problem that is mostly ignored by the SCM literature is the effect of having finite data and its role in the partial identification problem.

To address the finite sample problem, we propose a novel formulation for obtaining causal effect bounds that are valid with a given confidence level obtained from the dataset. We then demonstrate how these bounds can be utilized for causal decision-making. Our key observation is that, having access to only finitely many samples *renders any causal effect non-identifiable*, i.e., it cannot be uniquely computed. This extends the concept of partial identifiability to causal effects that would be identifiable had we given access to infinitely many samples. In Figure 1 (Top), even though the interventional distribution  $p(y|do(x))$  should be computed uniquely (top-left), but estimators fail to predict the correct estimate due to low sample size. We construct a bound (top-right) with distributions consistent with the empirical dataset to facilitate our decision-making.

Next, we extend our uncertainty-aware causal effect bounds to causal queries that are not identifiable even with infinite data. Interestingly, our formulation enables a very natural decomposition of the causal effect bounds into two categories: A range of causal effect values that are guaranteed not to shrink even if we increase the number of samples in our dataset, called the nonID region, and the rest that may be reduced by collecting more samples. In a causal decision-making scenario, this nonID region crucially helps us to decide the next move: collect more samples or observe more variables. In Figure 1 (bottom),  $p(y|do(x))$  is non-identifiable (bottom-left). The interval becomes wider due to finite samples (bottom-right). We decompose this wider bound into informative regions to suggest the next move.

Finally, to approximate these bounds, which are in general computationally challenging, we resort to using

neural/deep causal models (Balazadeh Meresht et al., 2022; Kocaoglu et al., 2018; Rahman and Kocaoglu, 2024; Xia et al., 2021). We show that the nonID causal effect region can be obtained by solving min-max and max-min problems. Outer optimization searches over observational distributions within a confidence set, and the inner optimization for a fixed distribution searches over all (neural) SCMs to maximize/minimize causal effect. Below are our contributions:

- To the best of our knowledge, we are the first to introduce a decision-making framework motivated by a surprising algorithmic discovery that it is possible to conclude with high probability that collecting more observational samples can not help with causal decision making. We establish a novel algorithm, UA-DCM, that decomposes the epistemic uncertainty into *nonID uncertainty* and *sample uncertainty*. The former can be reduced by accessing a more detailed account of the system, while the latter can be reduced by a larger number of samples.
- To obtain the interval decomposition for an arbitrary graph with discrete variables containing unobserved confounders, UA-DCM solves min-max and max-min problems by employing deep causal models.
- We demonstrate the utility of our algorithm through extensive experiments on synthetic data of various complexity and on the real-world parent labor dataset.

## 2 Background

**Definition 1** (Structural causal model (SCM) (Pearl, 2009)). An SCM  $S$  is a tuple of five elements:  $S = (\mathbf{V}, \mathcal{N}, \mathcal{U}, \mathcal{F}, P(\cdot))$ . Here, each observed variable  $V_i \in \mathbf{V}$  is realized as an evaluation of the function  $f_i \in \mathcal{F}$  by taking as input a subset of the remaining observed variables  $Pa_i \subset \mathbf{V}$ , an exogenous noise variable  $E_i \in \mathcal{N}$ , and optionally an unobserved confounding variable  $U_i \in \mathcal{U}$ .  $P(\cdot)$  is a product joint over all unobserved  $\mathcal{N} \cup \mathcal{U}$ . An SCM containing unobserved confounders is called a **Non-Markovian causal model**. A *causal graph*,  $G$ , representing the variables as nodes and structural functional relationships encoded in the SCM as edges, is called an Acyclic Directed Mixed Graph (ADMG) and denoted as  $S \models G$ .

**Definition 2** (Causal effect and do-intervention). A do-intervention  $do(x)$  replaces the functional equation  $X = f_X$  with a specific value  $X = x$  without affecting other equations. The distribution induced on the variable  $Y$  after such an intervention is called an interventional distribution  $P(Y|do(x))$ . With no intervention, the observational joint distribution of  $\mathbf{V}$  is  $P(\mathbf{V})$ . The average treatment effect (ATE) is defined for binary treatments as:  $ATE = \mathbb{E}[Y|do(X = 1)] - \mathbb{E}[Y|do(X = 0)]$ . For multiple actions, we define the ATE of an action  $X = x$  with respect to the best among remaining actions  $x_b$  as:  $ATE(x) = \mathbb{E}[Y|do(X = x)] - \max_{x_b \neq x} \mathbb{E}[Y|do(X = x_b)]$ .

**Definition 3** (Deep causal models (DCM) (Kocaoglu et al., 2018; Xia et al., 2021; Rahman and Kocaoglu, 2024)). A neural net architecture  $\mathbb{G}$  is called a deep causal model (DCM) for an ADMG  $G = (\mathbf{V}, \mathcal{E})$  if it consists of a collection of neural nets, one  $f_i$  (or interchangeably  $f_{V_i}$ ) for each  $V_i \in \mathbf{V}$  such that i) each  $f_i$  accepts a sufficiently high-dimensional noise vector  $N_i$ , ii) the output of  $f_j$  is input to  $f_i$  iff  $V_j \in Pa_G(V_i)$ , iii)  $N_i = N_j$  iff  $V_i, V_j$  share an unobserved confounder. Functions in DCM,  $\mathbb{G} = \{f_1, \dots, f_n\}$  are parameterized by  $\Theta = \{\theta_1, \dots, \theta_{|\mathcal{V}|}\}$ . Similar to the original data distribution,  $P(\mathcal{V})$ , we define  $P_\theta(\mathcal{V})$  to be the distribution induced by the DCM. Sufficiently high-dimensional noise vectors  $N_i$ , e.g., Gaussian, can replace both the exogenous noises and the unobserved confounders in the true SCM. We consider DCM to be *representative enough for an SCM* if the neural networks have sufficiently many parameters to induce the same observed distribution as the true SCM. When a latent confounder  $U$  affects two observed variables  $X$  and  $Y$ , we can match the joint distribution  $P(X, Y)$  by feeding the same prior noise  $N_X = N_Y$  (as confounders) into both neural architectures  $f_X, f_Y$ .

**Theorem 1.** (Kocaoglu et al., 2018; Xia et al., 2021; Rahman and Kocaoglu, 2024) Consider any SCM  $S = (\mathbf{V}, \mathcal{N}, \mathcal{U}, \mathcal{F}, P(\cdot))$ . A DCM  $\mathbb{G} = \{f_1, \dots, f_n\}$  for  $G$  entails the same identifiable interventional distributions as the SCM  $S$  if it entails the same observational distribution.

**Definition 4** (Causal effect with DCM). To perform a hard intervention  $do(X = x)$ , we manually set the values for the intervened variables as  $X = x$  instead of using their neural network. Then, we feed

forward those values into their children and the rest of the mechanisms will work as usual to generate their corresponding values from which we can estimate the causal effect  $P(y|do(x))$  and ATE. A loss function measuring  $d(P(\mathbf{V}, P_\theta(\mathbf{V}))$  can be used to train DCM’s end-to-end differentiable networks. When causal effects are not pointwise identifiable, we add an additional loss function to maximize or minimize the causal effects.

### 3 Related Work

When the causal effect is not identifiable, one can identify a range of causal effects from the SCMs that are compatible with the observational data. Tian and Pearl (2000) used the response variable to get bounds of counterfactual queries from observational and interventional data. Duarte et al. (2024) proposed an automated method to derive bounds for causal queries in arbitrary graphs. Many researchers have explored the use of neural nets Xia et al. (2021); Balazadeh Meresht et al. (2022); Rahman and Kocaoglu (2024) to design causal models and estimate causal queries by maximizing and minimizing the query under the semi-Markovian setting.

In the uncertainty quantification literature, Melnychuk et al. (2024) proposed a method for quantifying aleatoric uncertainty in individualized treatment effects by deriving sharp bounds on the conditional distributions of the treatment effect. Marmarelis et al. (2024) introduced an approach for constructing causal effect intervals with hidden confounding. Existing causal methods approach the decision-making problem from different perspectives. Frauen et al. (2023) proposed a neural framework for sensitivity analysis that is compatible with a large class of existing sensitivity models. Jesson et al. (2020) studied the decision-making problem under non-overlap. Frauen et al. (2025) propose an optimal decision-making approach with two-stage CATE estimators.

These approaches do not have the capability to disentangle the uncertainty in the causal effect bounds obtained from finite number of samples. Distributionally robust optimization (Bui et al., 2022; Gao and Kleywegt, 2023) performs a max-min or min-max optimization which has similarity to our method. However, while DRO searches for a model that is robust to distributions within an  $\epsilon$ -ball, we instead search for distributions within the ball that allows a model to achieve the best local minimum or the worst local maximum. Confidence intervals can be introduced to existing causal effect estimation methods using techniques like bootstrapping. Neither such confidence intervals nor causal effect bounds obtained by these methods can distinguish the uncertainty in the intervals and suggest a practitioner how to reduce it.

### 4 Causal Decision-Making with ID Queries

Between two possible interventions on a variable  $X$  (ex: taking/not taking a medicine), we can decide the best action by comparing their causal effect on the outcome  $Y$  (ex: recovery). For example, the action  $X = 1$  is better than  $X = 0$  if  $P(Y|do(X = 1)) > P(Y|do(X = 0))$ . When randomized trials are not possible, we need an estimation of an interventional query from observational data. The ID algorithm (Tian and Pearl, 2002; Shpitser and Pearl, 2008) provides us with a complete characterization of which causal queries can be uniquely answered from observational data. For example, in the backdoor graph of Figure 1 top-left, the effect of intervening on  $X$  on  $Y$  is identifiable through the backdoor formula:  $p(y|do(x)) = \sum_z p(y|x, z)p(z)$ . This means that with infinite samples, we can perfectly estimate the conditionals in the formula to evaluate this expression exactly. However, in practice, we do not have access to the joint distribution.

We propose using a confidence set of distributions that contains the true distribution with some specified error probability  $\alpha$ . Specifically, for a probability distribution  $P$ , the confidence region  $\mathcal{C}(\hat{P})$  is a random set such that  $\mathbb{P}(P \in \mathcal{C}(\hat{P})) \geq 1 - \alpha$ , where  $\mathbb{P}$  is the empirical measure induced by observing a given number of IID samples from  $P$ . There are various ways to construct a confidence set, extending on the classical confidence intervals. We use the simplest set defined as the cartesian product of intervals obtained via concentration inequalities in each coordinate of the joint distribution, given as follows:  $\mathcal{S} := \prod_{v \in \mathcal{V}} [l_v, u_v]$ , where  $v$  is a configuration of the joint variable set and  $l_v, u_v$  are the lower and upper bounds that contain true  $p(v)$  with probability  $\alpha/m$ , where  $m$  is the total number of configurations in the observed distributions. Thus,  $p \in \mathcal{S}$  with probability  $\alpha$  through a simple union bound argument.

The first question is, how does having a set of possible observational distributions change our knowledge of the causal effect? It turns out that this converts a pointwise identifiable query to an interval for the causal effect. We establish this through the following theorem:

**Theorem 2.** *Let  $f(P, S)$  be the estimand of an identifiable causal effect for SCM  $S$ , with the observational distribution  $P$ . Let  $\mathcal{P}$  be any connected set of observational distributions that contains  $P$ . Let  $a = \min_{P \in \mathcal{P}} f(P, S), b = \max_{P \in \mathcal{P}} f(P, S)$ . Then  $f|_{\mathcal{P}} : \mathcal{P} \rightarrow [a, b]$  is surjective.*

The proofs are provided in Section D.1 and Section D.2. In words, the collection of causal effects for a continuous set of observational distributions forms a contiguous interval in  $[0, 1]$ . This establishes that it is sufficient to obtain two numbers, one maximum causal effect and one minimum causal effect, to characterize this range of causal effect values. For certain graphs and queries, this problem can be solved easily, e.g., in the backdoor graph, the objective can be reduced to a linear program (section C.1).

For more general queries, this can be achieved through several existing methods. However, such optimization problems are hard to solve. For example, one can use the canonical SCM method which requires exponential space in general and solving very complicated polynomial programs. Alternatively, approximate heuristic solvers, such as Autobound (Duarte et al., 2024) can also be used. But they may take a long time to obtain meaningful bounds. We are the first to address this optimization problem with finite samples by proposing neural networks to simulate causal models, known in the literature as deep causal generative models (DCM) (Kocaoglu et al., 2018; Rahman and Kocaoglu, 2024) or neural causal models (Xia et al., 2021; Hu et al., 2021). The final output is the upper and lower bounds of the *identifiable* causal query, i.e.,  $[L, U]$ , created due to the finite sample uncertainty. We can decide action  $X = 1$  is better if  $[L_{x_0}, U_{x_0}]$  and  $[L_{x_1}, U_{x_1}]$  are separated and  $L_{x_1} > U_{x_0}$ .

## 5 Decomposing Causal Effect Uncertainty

In this section, we address non-identifiable queries under finite sample uncertainty. When the causal effect is uniquely identifiable from observational data, we can have pointwise estimation with infinite samples or bounds with finite samples. However, with unobserved confounders, even with infinite samples, we might not uniquely estimate the effect from observational data. This is known as a non-identifiable query: multiple SCMs consistent with the given causal graph and observational data, but with different causal effects. For a fixed causal graph and observational distribution, existing algorithms can be used to search the SCM space to find the maximum and minimum causal effect and construct a bound  $[L_x, U_x]$ . Finding these the two values:  $L_x, U_x$  is sufficient to characterize the range of causal effect values for a non-id query, as this bound is a continuous set and any value in this set can be achieved by some SCM with the same graph and observational distribution. Formally,

**Theorem 3.** *Let  $f(p, S)$  be the estimand of some non-identifiable causal effect of interest for some causal graph, and the observational distribution  $p$ . Let  $\mathcal{S}$  be the set of the SCM such that  $P_{obs}(S) = p$ . Let  $a = \min_{S \in \mathcal{S}} f(p, S), b = \max_{S \in \mathcal{S}} f(p, S)$ . Then  $f|_p : \mathcal{S} \rightarrow [a, b]$  is surjective.*

If the best decision cannot be determined from the bounds of causal effect, a possible next step is to collect more samples to improve the confidence of our estimations. However, for the non-identifiable causal query, even in the limit of infinite data, the bounds of causal effects from two actions may still overlap. In that case, one would need to resort to other approaches, such as utilizing additional variables.

We specify the process of reaching to the final decision through a sequence of three moves: *i*) we **return** the best action (shown as  $\checkmark$ ), *ii*) we can not decide yet but conclude that no amount of data points would disambiguate the causal effect. Thus, we must **observe** additional variables, *iii*) we can not decide yet but it is possible that collecting more data points can disambiguate the causal effect. Thus, we **collect** more samples. The main question we pose in this paper is that: *Can we ever know whether collecting more samples will never lead to informed decision-making?* To answer this question, we need to gain insight into two different types of epistemic uncertainty without knowing the observational distribution exactly: one modeling uncertainty due to unobserved confounding, and one modeling the uncertainty due to finite samples. Our proposed method distinguishes between the two uncertainties by providing a lower bound for the uncertainty that cannot be reduced by collecting more samples. This helps us decide the right conclusion about data

collection practices for decision-making. In the next section, we introduce sample and nonID uncertainty for single and multiple actions.

**Assumptions:** We assume *i*) discrete variables , *ii*) Semi-Markovian SCM and *iii*) access to the acyclic directed mixed graph (ADMG). See Section D for details.

## 5.1 Decision Making with single action

In many scenarios, we need to compare the bounds of the causal effect  $P(y|do(x))$  with a scalar quantity such as the marginal  $P(y)$ . Suppose we need to make the critical decision of choosing an action  $X = x$  for the population level to improve the outcome. We can determine that by comparing the bound of  $P(Y|do(x))$  with the probability  $P(Y)$ : the model is biased if  $P(Y) \notin [minP(Y|do(x)), maxP(Y|do(x))]$  for a specific  $x$ . Below, we specify the uncertainty for any specific action and the decision-making based on that.

**Definition 5** (sample and nonID Uncertainty (Figure 2)). *Let an empirical estimation of the joint distribution  $P$  be  $\hat{P}$  and a confidence set  $\mathcal{C}$  be such that  $\mathcal{C}$  covers the true  $P$  with probability of at least  $1 - \alpha$ . Define the set  $\mathcal{S}_P = \{S \text{ an SCM} \mid P_{obs}(S) = P, S \models G\}$  and  $\mathcal{I}_P = \{P_S(y|do(x)) \mid S \in \mathcal{S}_P\}$ . Then define the intersection  $\bigcap_{P \in \mathcal{C}} \mathcal{I}_P$  to be the **nonID uncertainty**, and the set difference  $\bigcup_{P \in \mathcal{C}} \mathcal{I}_P \setminus \bigcap_{P \in \mathcal{C}} \mathcal{I}_P$  to be the **sample uncertainty**. The epistemic uncertainty region in the estimation would be the union of these subcomponents. The components are named the inner region and the outer band, respectively.*

**Proposition 1.** *The uncertainty in the causal decision-making problem due to nonID uncertainty in  $P(y|do(x))$  (i.e., inner region) cannot be reduced by increasing the number of samples in the data.*

**Proposition 2.** *There exists SCMs  $S \in \mathcal{S}_P$  where the uncertainty in the causal decision-making problem due to sample uncertainty in  $P(y|do(x))$  (i.e., outer band) can be reduced by increasing the number of samples in the data.*

**Definition 6** (Inner region:  $[\bar{L}_x, \bar{U}_x]$ , Outer band  $[\underline{L}_x, \bar{L}_x] \cup [\bar{U}_x, \bar{U}_x]$ ). *Given a confidence set  $\mathcal{C}$  of an empirical distribution  $\hat{P}$ , Define the set  $\mathcal{S}_P = \{S \text{ an SCM} \mid P_{obs}(S) = P, S \models G\}$ . We access the sample and non-id uncertainty regions by estimating the following quantities:*

$$\begin{aligned} \bar{U}_{do(x)} &:= \max_{P \in \mathcal{C}(\hat{P})} \max_{S \in \mathcal{S}_P} P_S(Y|do(X = x)) \\ \underline{U}_{do(x)} &:= \min_{P \in \mathcal{C}(\hat{P})} \max_{S \in \mathcal{S}_P} P_S(Y|do(X = x)) \\ \bar{L}_{do(x)} &:= \max_{P \in \mathcal{C}(\hat{P})} \min_{S \in \mathcal{S}_P} P_S(Y|do(X = x)) \\ \underline{L}_{do(x)} &:= \min_{P \in \mathcal{C}(\hat{P})} \min_{S \in \mathcal{S}_P} P_S(Y|do(X = x)), \end{aligned} \tag{1}$$

**Theorem 4.** *Given a confidence set,  $\mathcal{C}$  and a set of causal effects,  $\mathcal{I}_P$  (Def. 5),  $\bigcap_{P \in \mathcal{C}} \mathcal{I}_P = [\bar{L}_{do(x)}, \underline{U}_{do(x)}]$ .*

**Corollary 1.** *Given a confidence set,  $\mathcal{C}$  and a set of causal effects,  $\mathcal{I}_P$  (Def. 5), we have  $\bigcup_{P \in \mathcal{C}} \mathcal{I}_P \setminus \bigcap_{P \in \mathcal{C}} \mathcal{I}_P = [\underline{L}_{do(x)}, \bar{L}_{do(x)}] \cup [\underline{U}_{do(x)}, \bar{U}_{do(x)}]$*

**Definition 7.** *An causal decision based on  $P(y|do(x))$  bound and  $\gamma = P(y)$  is ambiguous given confidence set  $\mathcal{C}$  if there exists two SCMs  $S_1, S_2$  where  $p_{S_1}(y_1|do(x)) > \gamma$  and  $p_{S_2}(y_1|do(x)) < \gamma$  where  $S_1, S_2$  entail  $p_1, p_2 \in \mathcal{C}$ .*

**Theorem 5.** *For a causal decision making problem with  $P(y|do(x))$  bound, let  $(\bar{U}_{do(x)}, \underline{U}_{do(x)}, \bar{L}_{do(x)}, \underline{L}_{do(x)})$ , and  $\gamma = P(y)$  be estimated from the data. The decision is unambiguous if  $\underline{L}_{do(x)} > \gamma$  or  $\gamma > \bar{U}_{do(x)}$ . The decision is unidentifiable and cannot be improved with more data if  $\bar{L}_x < \gamma < \underline{U}_{do(x)}$ .*

Note that  $\gamma = P(y)$  can be provided by a domain expert. If we estimate it from data, the framework for multiple actions discussed in the next section can be utilized to make a decision in such cases.

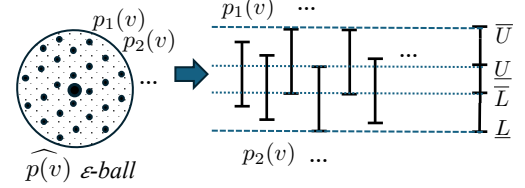


Figure 2: The proposed inner and outer causal effect bounds.

## 5.2 Decision making with multiple actions:

In this section, we consider a scenario in which we compare the effects of multiple (two or more) actions to choose the best action. We utilize the quantity average treatment effect (ATE) instead of  $P(y|do(x))$  for decision making.

**Definition 8** (sample and nonID Uncertainty (Figure 2)). *Let an empirical estimation of the joint distribution  $P$  be  $\hat{P}$  and a confidence set  $\mathcal{C}$  be such that  $\mathcal{C}$  covers the true  $P$  with probability of at least  $1 - \alpha$ . Define the set  $\mathcal{S}_P = \{S \text{ an SCM} \mid P_{obs}(S) = P, S \models G\}$  and  $\mathcal{I}_P(x) = \{\text{ATE}(x) \mid S \in \mathcal{S}_P\}$ . Then define the intersection  $\bigcap_{P \in \mathcal{C}} \mathcal{I}_P$  to be the **nonID uncertainty**, and the set difference  $\bigcup_{P \in \mathcal{C}} \mathcal{I}_P \setminus \bigcap_{P \in \mathcal{C}} \mathcal{I}_P$  to be the **sample uncertainty**. The total epistemic uncertainty region in the estimation would be the union of these two subcomponents.*

**Proposition 3.** *The uncertainty in the causal decision-making due to nonID uncertainty in  $\text{ATE}(x)$  cannot be reduced by increasing the sample size.*

**Proposition 4.** *There exists SCMs  $S \in \mathcal{S}_P$  where the uncertainty in the causal decision making problem due to sample in  $\text{ATE}(x)$  can be reduced by increasing the number of samples in the data.*

**Definition 9** (Inner ate bound:  $[\underline{L}_{ate}, \overline{U}_{ate}]$ , Outer ate band  $[\underline{L}_{ate}, \overline{L}_{ate}] \cup [\underline{U}_{ate}, \overline{U}_{ate}]$ ). *Given a confidence set  $\mathcal{C}$ , we access the sample and non-id uncertainty regions by estimating four quantities for ATE same as Definition 6. See Def 12 in the appendix for details.*

**Theorem 6.** *Given a confidence set  $\mathcal{C}$  and ATE values  $\mathcal{I}_P$  (Def. 8),  $\bigcap_{P \in \mathcal{C}} \mathcal{I}_P = [\underline{L}_{ate_x}, \overline{U}_{ate_x}]$ .*

**Corollary 2.** *Given a confidence set,  $\mathcal{C}$  and a set of average treatment effect values,  $\mathcal{I}_P$  (Def. 8), we have  $\bigcup_{P \in \mathcal{C}} \mathcal{I}_P \setminus \bigcap_{P \in \mathcal{C}} \mathcal{I}_P = [\underline{L}_{ate_x}, \overline{L}_{ate_x}] \cup [\underline{U}_{ate_x}, \overline{U}_{ate_x}]$*

**Definition 10.** *An causal decision with  $\text{ATE}(x)$  as decision metric is ambiguous given confidence set  $\mathcal{C}$  if for any action  $x \in \mathcal{X}$ , there exists two SCMs  $S_1, S_2$  entailing  $p_1, p_2 \in \mathcal{C}$  with best actions  $x_{b_1}, x_{b_2}$  in  $\mathcal{X} \setminus \{x\}$  such that  $\text{ATE}_{S_1}(x, x_b) > 0$  and  $\text{ATE}_{S_2}(x, x_b) < 0$ .*

**Theorem 7.** *For a causal decision-making problem with  $\text{ATE}(x)$  as the decision metric, let  $(\overline{U}_{ate_x}, \underline{U}_{ate_x}, \overline{L}_{ate_x}, \underline{L}_{ate_x})$  be estimated from the data. The decision of  $X = x$  as the best action (or cannot be the best action) is unambiguous if  $\underline{L}_{ate_x} > 0$  (or  $\overline{U}_{ate_x} < 0$ ). The decision is ambiguous and cannot be improved with more data if  $\underline{L}_{ate_x} < 0 < \overline{U}_{ate_x}$ .*

**From ambiguous to unambiguous decision:** As previously mentioned, we reach the final decision through a sequence of three moves. Let  $\gamma = \{P(y), 0\}$ . 1. *Return:* if  $\gamma \notin [\underline{L}_{do(x)}, \overline{U}_{do(x)}]$ , we decide the action is beneficial in population level. For multiple actions, if  $0 \notin [\underline{L}_{ate_x}, \overline{U}_{ate_x}]$  then we return  $do(X = x)$  as the best action. 2. *Observe:* if  $\overline{L}_x < \gamma < \underline{U}_x$ , then we observe additional variables for example instrument variables. Observing additional variables gives us a small causal effect set  $\mathcal{I}'_P$ , for each  $P \in \mathcal{C}$ . Thus, for fixed  $\mathcal{C}$ , we get a narrower inner region,  $[\overline{L}_x, \underline{U}_x] = \bigcap_{P \in \mathcal{C}} \mathcal{I}'_P$  and a narrower/wider outer band,  $[\underline{L}_x, \overline{L}_x] \cup [\underline{U}_x, \overline{U}_x] = \bigcup_{P \in \mathcal{C}} \mathcal{I}'_P \setminus \bigcap_{P \in \mathcal{C}} \mathcal{I}'_P$ . Also, the average non-id bound width will reduce since  $1/|\mathcal{C}| \sum_{P \in \mathcal{C}} |\mathcal{I}'_P| \leq 1/|\mathcal{C}| \sum_{P \in \mathcal{C}} |\mathcal{I}_P|$ . 3. *Collect:* In all other scenarios, we are unsure about the source of uncertainty (low sample size or non-identifiability) and we collect more samples, with the assumption that obtaining samples with additional variables is more challenging compared to collecting samples of the same set of variables. More samples provides us a smaller confidence set  $\mathcal{C}'(\hat{P})$ . Thus, according to Theorem 4 and 6, we get a wider inner region,  $[\overline{L}_x, \underline{U}_x] = \bigcap_{P \in \mathcal{C}'} \mathcal{I}_P$  and according to Corrolary 1 and 2, a narrower outer band,  $[\underline{L}_x, \overline{L}_x] \cup [\underline{U}_x, \overline{U}_x] = \bigcup_{P \in \mathcal{C}'} \mathcal{I}_P \setminus \bigcap_{P \in \mathcal{C}'} \mathcal{I}_P$ . The *collect* and *observe* moves can continue until we reach the *return* move and decide the best action.

## 5.3 DCM for estimating sample and nonID uncertainty

In this section, we introduce three algorithms. Algorithm 1 calls Algorithm 2 to construct the  $\epsilon$ -net and then executes Algorithm 3: RelaxedDCM for each distribution in the  $\epsilon$ -net to find the non-id causal effect bound. Finally, Alg. 1: Explore  $\epsilon$ -ball combines these bounds to construct the inner and outer band  $[\underline{L}_x, \overline{L}_x, \underline{U}_x, \overline{U}_x]$  to decide the next move.

---

**Algorithm 1** Explore  $\epsilon$ -ball

---

```

1: Input: data  $\{\mathbf{v}_k\}_{k=1}^n$ , graph  $\mathcal{G}$ , small interval  $\epsilon_s$ 
2: Output: Decision/Collect/Observe
3: Initialize  $\gamma = P(y)$  for single action and  $\gamma = 0$  for multiple actions (ATE).
4: while Not Decided do
5:   Candidates = Construct  $\epsilon$ -net(data,  $\mathbf{V}, \epsilon_s$ )
6:   for  $P_\epsilon(\mathbf{V}) \in$  Candidates do
7:     for  $x$  in  $sup(X)$  do
8:        $\underline{U}_x, \overline{U}_x \leftarrow$  RelaxedDCM(data,  $\mathbf{V}, \mathcal{G}, X = x, \epsilon_s$ )
9:        $\overline{U}_x, \underline{U}_x = \max(\overline{U}_x, U_x), \min(\underline{U}_x, U_x)$ 
10:       $\underline{L}_x, \overline{L}_x = \min(\underline{L}_x, L_x), \max(\overline{L}_x, L_x)$ 
11:      if  $\gamma \notin [\underline{L}_x, \overline{U}_x]$  then
12:        Return  $X = x$  as conclusive/  $do(x)$  is better/worse compared to  $P(y)$ 
13:      else if  $\gamma \in [\underline{L}_x, \underline{U}_x]$  then
14:        Observe variables
15:      else if  $\gamma \in [\underline{L}_x, \overline{L}_x] \cup [\underline{U}_x, \overline{U}_x]$  then
16:        Collect more samples

```

---

**Algorithm 2** Construct  $\epsilon$ -net

---

```

1: Input: data  $\{\mathbf{v}_k\}_{k=1}^n$ , Variable set  $\mathbf{V}$ , graph  $\mathcal{G}$ , small interval  $\epsilon_s$ 
2: Factorize  $\hat{P}(\mathbf{v})$  in  $\Pi_{v \in \mathbf{V}} \hat{P}(v_i | v^{\pi_i-1})$ 
3: for each  $V_i \in \mathbf{V}$  do
4:    $\epsilon = \sqrt{\frac{\ln(2/\alpha)}{2n}}$  where  $n = count(D[v^{\pi_i-1}])$ 
5:    $C_i = \lceil \epsilon/\epsilon_s \rceil$  equidistance points in  $\hat{P}_n(v_i = 1 | v^{\pi_i-1}) \pm \epsilon$ 
6: Sample  $m$  joints s.t.  $\{(p_1^{(j)}, \dots, p_{|\mathbf{V}|}^{(j)})\}_{j=1}^m \subseteq C_1 \times C_2 \times \dots \times C_{|\mathbf{V}|}$ 
7: Return  $m$  candidate joint distributions.

```

---

**Algorithm 3: Optimizing Relaxed-DCM:** Given a fixed distribution  $P_\epsilon$ , in Alg. 3, we train deep causal models (see Def. 3) to learn  $P_\epsilon$  while optimizing the causal effects. Unlike existing works that attempt to match  $P_\epsilon$  exactly, we use a Lagrangian duality-based optimization (Bui et al., 2022; Gao and Kleywegt, 2023) to keep the observational distribution entailed by the DCM  $P_\theta$ , within a small region around input distribution,  $P_\epsilon$  (Alg 3: line 7). The dual update parameter successfully finds the right amount of regularization and maintains the desired distributional distance (Alg 3: line 9). We add the causal effect magnitude with the distributional loss terms and optimize the parameters to maximize or minimize the effects (Alg 3: lines 8, 10).

**Algorithm 2: Construct  $\epsilon$ -net :** Since the given dataset might be sampled from any distribution in the confidence set  $\mathcal{C}$  of the empirical distribution  $\hat{P}$ , we need to solve the max-max, max-min, min-max and min-min problems (Equation 1, 2) by searching over  $\mathcal{C}$ . To obtain the confidence set in practice, we factorize the empirical distribution  $\hat{P}(\mathbf{v})$  into conditional distributions, i.e.,  $\hat{P}(\mathbf{v}) = \Pi_{v \in \mathbf{V}} \hat{P}(v_i | v^{\pi_i-1})$  and construct non-asymptotic confidence interval for variable with  $m$  total number of configurations, from  $n$  samples w/ error probability  $\alpha = 0.05m$ , using Hoeffding inequality (Hoeffding, 1963) and Bonferroni correction, i.e.,  $\hat{P}_n(v_i = 1 | v^{\pi_i-1}) \pm \sqrt{\frac{\ln(2/\alpha)}{2n}}$ . See Appendix C.3 for derivation. If we pick one point from each interval to form a joint distribution and optimize the causal effect, we obtain the maximum and minimum effect for that specific distribution. To obtain the four quantities in Equation 1, 2, we have to search over all constructed intervals and optimize the causal effect while matching each formed distribution.

Note that solving a max-min and min-max problem by searching over these confidence intervals is not convex in general. To address this scenario, we resort to a heuristic approach motivated from  $\epsilon$ -net (Gonzalez, 1985). To implement  $\epsilon$ -net, we have to cover the metric space of observational distributions  $M$  consistent with the input dataset, with open balls having centers in  $X \subset M$  such that every distribution in  $M$  is within  $\epsilon$  distance of at least one distribution in  $X$ . For our purpose, we cover each confidence intervals with smaller intervals of width  $\epsilon_s$ . If  $\epsilon$  is the interval width, this would give us  $\lceil \epsilon/\epsilon_s \rceil$  number of centroids. We pick centroid for each conditional and form a joint distribution. After optimizing the DCM for these distributions, we take the minimum (or maximum) of all optimized values to approximate the minmax (or maxmin).

Note that the number of confidence intervals increases with the support size and the number of variables. If we consider  $\lceil \epsilon/\epsilon_s \rceil$  centroids in each interval, the number of all possible joint distributions will be extremely high. To deal with such a scenario, we uniformly pick a centroid from each conditional distribution interval

---

**Algorithm 3** RelaxedDCM Training Model

---

```

1: Input: data  $\{\mathbf{v}_k\}_{k=1}^n$ , Variables  $\mathbf{V}$ , graph  $\mathcal{G}$ , action  $x$ , smaller interval  $\epsilon_s$ 
2: Initialize DCM parameters  $\Theta_{\min} \leftarrow \{\theta_i\}_{V_i \in \mathbf{V}}$  and  $\Theta_{\max} \leftarrow \{\theta_i\}_{V_i \in \mathbf{V}}$ 
3: Initialize dual parameter  $\beta$  and ate weight  $\lambda$ .
4: for  $j \in [0, 1]$  ▷ 0: minimization, 1: maximization do
5:   for  $epoch = 1 \rightarrow max\_epoch$  do
6:      $d_i = dist(P_\epsilon(v_i \mid v_{\pi(i-1)}), P_{\Theta_i}(v_i \mid v_{\pi(i-1)}))$ ,  $\forall_i : V_i \in \mathbf{V}$ 
7:      $L \leftarrow \frac{1}{n} \sum_{k=1}^n \sum_{V_i \in \mathbf{V}} \alpha_i [d_i - \epsilon_s]$ 
8:      $\mathcal{L} \leftarrow L + (-1)^j * \lambda \log ATE^{(\Theta)}(x, x_b)$ 
9:      $\alpha_i \leftarrow \max(0, \alpha_i + lr \cdot (d_i - \epsilon_s))$ ,  $\forall_i : V_i \in \mathbf{V}$ 
10:     $\Theta \leftarrow \Theta - \eta \nabla \mathcal{L}$ 

```

---

and form a valid joint distribution  $P$ . For a binary two variable case  $X, Y$ , we can split the CI of  $P(X = 1)$  into  $n + 1$  smaller intervals by placing  $n$  centroids. We pick uniformly a value  $p$  from these  $n$  centroids having  $P(X = 0) = 1 - p$ . Doing the same for  $P(Y = 1|X = 0)$  and  $P(Y = 1|X = 1)$  will allow us to construct  $P(X, Y)$ . However, since we are sampling the joint distribution only a finite number of times, it is possible that we miss the true distribution. We have to accept a small error in the constructed bounds  $[\underline{L}_x, \bar{L}_x, \underline{U}_x, \bar{U}_x]$  as well. We leave the development of better search strategies for future work. While exploring the confidence interval, if a candidate distribution becomes inconsistent with the assumed instrument graph, we reject it based on conditions proposed in (Pearl, 2013). Finally, our algorithm can deal with positivity violation of any distribution by considering the whole region  $[0, 1]$  as its confidence interval.

**Algorithm 1: Explore  $\epsilon$ -ball :** After collecting  $[\underline{L}_x, \bar{U}_x]$  bounds from each distribution in the confidence interval, we follow Equation 1 or 2 to obtain the inner  $[\underline{L}_x, \bar{U}_x]$  region and the outer  $[\underline{L}_x, \bar{L}_x] \cup [\underline{U}_x, \bar{U}_x]$  band. If the bounds are completely separated for  $do(x_0)$  and  $do(x_1)$ , we return the best action (Alg 1, line: 12). If the inner region intersects, we conclude with high probability that additional variables must be observed (Alg 1, line: 14). In this paper, we suggest observing instrument variables  $I$  (s.t.  $I \rightarrow X$ ) since it is theoretically established in literature that an instrument can reduce the non-id region (Neuberg, 2003; Balke and Pearl, 1996). Whether other variables can reduce the causal effect bounds is an open area to explore. In all other cases, we conclude collecting more samples (Alg 1, line: 16). The conclusion is with high probability as it depends on how correctly we approximated the  $\epsilon$ -net and explored it and how well we optimized the neural networks. Additional details about the algorithm are included in section E.4.

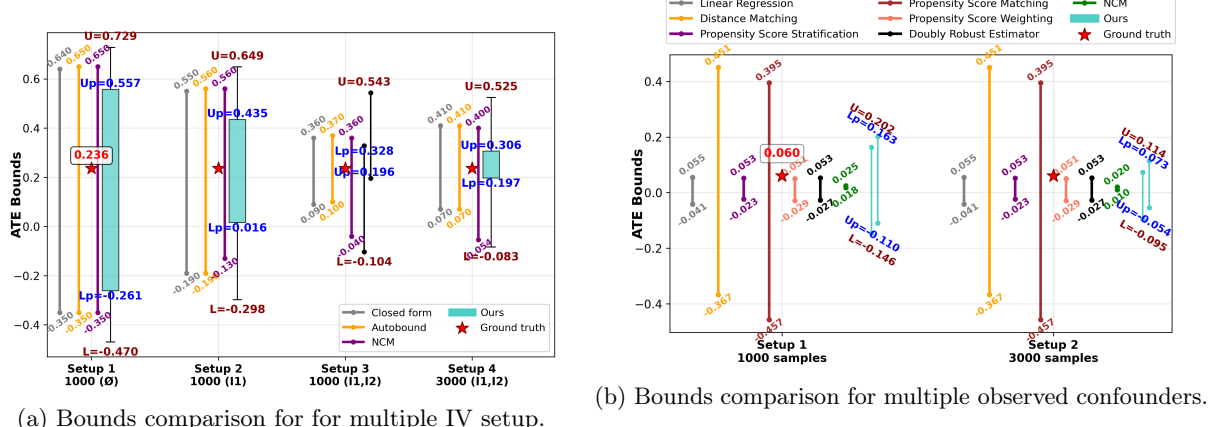
## 6 Experimental Analysis

In this section, we discuss the empirical evaluation of our algorithm on two synthetic and one real-world dataset and compare our performance with multiple baselines. We show the value of our approach by illustrating how it can be utilized sequentially for decision-making. We also demonstrate that the existing baselines may incorrectly declare the best action, whereas we can not only conclude that choosing the best action is impossible, but also suggest whether we should collect more samples or observe more variables.

**Setup:** In all setups, we arrange the neural networks according to the given causal graph, such as a bow graph or an IV graph: bow with an instrument (Figure 5). We create confidence intervals for each conditional distributions from given samples and build the epsilon net. We sampled  $> 150$  distributions from the epsilon-net and generated 5000 samples to train the neural nets on each distribution. We recorded the lower and upper bounds which gives us the  $[\underline{L}_x, \bar{L}_x, \underline{U}_x, \bar{U}_x]$  for  $do(X = x)$  or  $ATE(x)$ .

### 6.1 SCM 1 (UA-DCM correctness & utility):

**Results:** In Figure 3a, we show the next moves and consequences of our algorithm for different sample sizes. In setup 1, for  $N = 1000$  samples of  $D[X, Y]$ , we observed that all three baselines, i.e., closedform, autobound and NCM output similar ATE bounds:  $[-0.35, 0.64]$ . They estimate  $P(X, Y)$  from data and use it as the true distribution to calculate the bounds. These baselines only indicate that the true ATE lies within a large bound but provide no additional information on how to reduce their bounds to make the best action decision. On the other hand, in UA-DCM, since  $\gamma \in [\bar{L}_{ate}, \bar{U}_{ate}]$ , i.e.,  $0 \in [-0.261, 0.557]$ , we conclude that we must *observe* additional variables. Additional samples will not reduce the intersection.



We illustrate the consequence of observing additional variables in setup 2 where we consider an additional instrument variable. We observe that for 1000 samples of  $D[I_1, X, Y]$ , all baselines bounds reduce to  $[-0.19, 0.56]$ . For UA-DCM, both the inner region and the outer band shrink, especially the inner bound from  $[-0.261, 0.557] \rightarrow [0.016, 0.435]$  indicating the reduction in the non-id region. However, as the solid region  $[\underline{L}_{ate}, \overline{U}_{ate}]$  does not contain 0, we do not know if the current uncertainty is due to unobserved confounders or low sample size. Thus, based on the feasibility of the setup, we have to select the next move. For our experiment, we conclude, *observing* another instrument  $I_2$ .

In setup 3, we show bounds obtained from all baselines and our algorithm UA-DCMfor 1000 samples of the dataset  $D[I_1, I_2, X, Y]$ , and in setup 4, we show results when we collect 3000 samples. In setup 3, the bounds reduce significantly while changing slightly in setup 4. UA-DCMfinally says that the outer band is  $[-0.083, 0.197]$ , which is very close to zero. Thus, collecting more samples will reveal that  $do(X = 1)$  is a better action compared to  $do(X = 0)$ .

## 6.2 SCM 2 (Sensitive setup):

We consider 2 observed confounders and no unobserved confounder (Figure 5c). Thus no uncertainty from non-identifiability. We compare with 6 baselines which are designed to provide point-wise estimations. To be fair, we perform bootstrapping and obtain bounds from them. We also compare with NCM which outputs ATE bound.

**Results:** We observe that for 1000 samples, distance matching and propensity score matching output a very wide bound, ex:  $[-0.457, 0.395]$ . Other baselines provide tighter bounds and NCM outputs  $[0.018, 0.025]$ . All of these methods estimate a probability table from the input 1000 samples and estimate the causal effect based on that. Even with bootstrapping, some of the bounds do not contain the true ATE = 0.06. As most of the baselines contain 0 within it, they suggest that no action can be decided as the better one. No other insight about uncertainty reduction can be extracted from them. On the other hand, UA-DCMprovides an outer bound  $[-0.14, 0.20]$  for 1000 samples and an outer bound  $[-0.09, 0.11]$  for 3000 samples. This indicates that the ATE obtained from the true distribution will be contained in this bound. Also, note that there is no gap between  $\underline{U}_{ate}$  and  $\overline{L}_{ate}$  ( $Up, Lp$ ), which implies that there is no non-id uncertainty here, hinting us to collect more samples.

## 6.3 Real Data Experiments: Parents' Labor Supply

**Setup:** We apply our algorithm on the Parents' Labor Supply dataset(Angrist and Evans, 1996) which contains contains 92k family records of their demographic and work details. Here, the goal is to evaluate the causal effect of having more than two children (treatment  $X$ :yes/no) on mother's labor supply (outcome  $Y$ : working or not) with respect to the population, i.e.,  $P(y = 1|do(x = 1))$  vs  $P(y = 1)$ . We follow (Angrist and Evans, 1996) and consider whether first two children are of same sex or not as an instrument variable  $I$  since this significantly motivates people to have the third child. We illustrate our algorithm performance on 1000, 2000 and 92k (full dataset) with and without an instrument.

**Algorithm execution:** In the experiment, we arrange the neural networks according to the bow graph i.e., the graph shown in Figure 5a. In the second experiment, we considered the "same sex children" as the instrument variable  $I$  and arranged the neural networks according to Figure 5b. For each graph, we illustrate our algorithm performance on 1000, 2000 and 92k (full dataset). We create confidence intervals for each conditional distributions from these samples and build the epsilon net. We sampled  $> 130$  distributions from the epsilon-net and generate 5000 samples to train the neural networks on each distribution. We recorded the lower and upper bounds which gives us the  $[\underline{L}_x, \bar{L}_x, \underline{U}_x, \bar{U}_x]$  for  $do(X = 1)$ . We also report the inner and outer bands, and finally, we present the average of all non-ID regions.

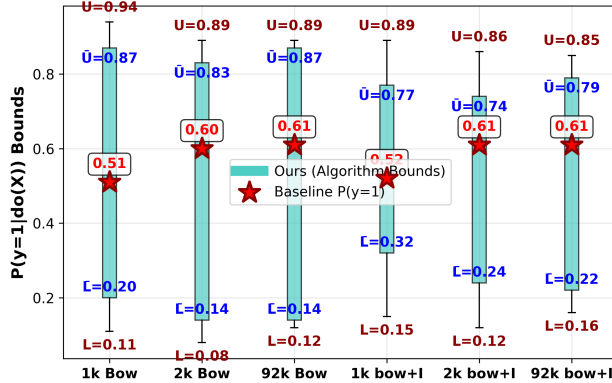


Figure 4: Experiment Results on Parents Labor Supply Dataset

*Consequence of collecting samples:* For the Bow graph, width of the inner region (cyan) of  $do(X = 1)$ ,  $[\bar{L}_x, \bar{U}_x]$ , expands as  $0.67 \rightarrow 0.69 \rightarrow 0.73$ , and the outer band  $[\underline{L}_x, \bar{L}_x] \cup [\underline{U}_x, \bar{U}_x]$  shrinks as  $0.16 \rightarrow 0.12 \rightarrow 0.04$ . For the Bow+instrument graph, the inner region of  $do(X = 1)$ ,  $[\bar{L}_x, \bar{U}_x]$ , expands as  $0.45 \rightarrow 0.50 \rightarrow 0.57$ , and the outer band  $[\underline{L}_x, \bar{L}_x] \cup [\underline{U}_x, \bar{U}_x]$  shrinks as  $0.29 \rightarrow 0.24 \rightarrow 0.12$ . This is consistent with the consequences of collecting more samples, as discussed in Section 5.

*Consequence of observing instrument:* The consequence becomes apparent when we look at the change in the *Non-id Region*. For  $do(X = 1)$  with 1000 samples, this region width reduces from  $0.67 \rightarrow 0.45$  when moving from the Bow graph to the Bow+ $I$  graph. Similarly, for 92k samples, the non-id region reduces from  $0.73 \rightarrow 0.57$  when moving from the Bow graph to the Bow+ $I$  graph. This implies that, the non-id region for each distribution has reduced due to observing the instrument variable.

## 7 Conclusion

We proposed a novel decomposition of epistemic uncertainty in causal effect estimation from finite data. We show that our decomposition can be used to conclude collecting more samples will not help with deciding the best action. We develop a neural net-based approach to approximate this decomposition in practice.

## Acknowledgements

This research has been supported in part by NSF CAREER 2239375, IIS 2348717, Amazon Research Award, Adobe Research and Intuit AI Research.

## References

Joaquín Abellán, George J Klir, and Serafín Moral. Disaggregated total uncertainty measure for credal sets. *International Journal of General Systems*, 35(1):29–44, 2006.

Joshua Angrist and William N Evans. Children and their parents' labor supply: Evidence from exogenous variation in family size, 1996.

Vahid Balazadeh Meresht, Vasilis Syrgkanis, and Rahul G Krishnan. Partial identification of treatment effects with implicit generative models. *Advances in Neural Information Processing Systems*, 35:22816–22829, 2022.

Alexander Balke and Judea Pearl. Counterfactual probabilities: Computational methods, bounds and applications. In *Uncertainty in artificial intelligence*, pages 46–54. Elsevier, 1994.

Alexander Balke and Judea Pearl. Bounds on treatment effects from studies with imperfect compliance. *Journal of the American statistical Association*, 92(439):1171–1176, 1997.

Alexander Balke and Judea Pearl. Probabilistic evaluation of counterfactual queries. In *Probabilistic and causal inference: The works of Judea Pearl*, pages 237–254. 2022.

Alexander A Balke and Judea Pearl. Universal formulas for treatment effects from noncompliance data. In *Lifetime data: models in reliability and survival analysis*, pages 39–43. Springer, 1996.

Patrick Blöbaum, Peter Götz, Kailash Budhathoki, Atalanti A. Mastakouri, and Dominik Janzing. Dowhy-gcm: An extension of dowhy for causal inference in graphical causal models. *Journal of Machine Learning Research*, 25(147):1–7, 2024. URL <http://jmlr.org/papers/v25/22-1258.html>.

Tuan Anh Bui, Trung Le, Quan Tran, He Zhao, and Dinh Phung. A unified wasserstein distributional robustness framework for adversarial training. *arXiv preprint arXiv:2202.13437*, 2022.

Patrick Chao, Patrick Blöbaum, Sapan Patel, and Shiva Prasad Kasiviswanathan. Modeling causal mechanisms with diffusion models for interventional and counterfactual queries. *arXiv preprint arXiv:2302.00860*, 2023.

Brian Cho, Dominik Meier, Kyra Gan, and Nathan Kallus. Reward maximization for pure exploration: Minimax optimal good arm identification for nonparametric multi-armed bandits. *arXiv preprint arXiv:2410.15564*, 2024.

Guilherme Duarte, Noam Finkelstein, Dean Knox, Jonathan Mummolo, and Ilya Shpitser. An automated approach to causal inference in discrete settings. *Journal of the American Statistical Association*, 119(547):1778–1793, 2024.

Benjamin Eva and Reuben Stern. Causal explanatory power. *The British Journal for the Philosophy of Science*, 2019.

Carlos Fernández-Loría and Foster Provost. Causal decision making and causal effect estimation are not the same... and why it matters. *INFORMS Journal on Data Science*, 1(1):4–16, 2022.

Dennis Frauen, Fergus Imrie, Alicia Curth, Valentyn Melnychuk, Stefan Feuerriegel, and Mihaela van der Schaar. A neural framework for generalized causal sensitivity analysis. *arXiv preprint arXiv:2311.16026*, 2023.

Dennis Frauen, Valentyn Melnychuk, Jonas Schweisthal, Mihaela van der Schaar, and Stefan Feuerriegel. Treatment effect estimation for optimal decision-making. *arXiv preprint arXiv:2505.13092*, 2025.

Yarin Gal et al. Uncertainty in deep learning. *phd thesis, University of Cambridge*, 2016.

Rui Gao and Anton Kleywegt. Distributionally robust stochastic optimization with wasserstein distance. *Mathematics of Operations Research*, 48(2):603–655, 2023.

Teofilo F Gonzalez. Clustering to minimize the maximum intercluster distance. *Theoretical computer science*, 38:293–306, 1985.

Wassily Hoeffding. Probability inequalities for sums of bounded random variables. *Journal of the American Statistical Association*, 58(301):13–30, 1963.

Stephen C Hora. Aleatory and epistemic uncertainty in probability elicitation with an example from hazardous waste management. *Reliability Engineering & System Safety*, 54(2-3):217–223, 1996.

Yaowei Hu, Yongkai Wu, Lu Zhang, and Xintao Wu. A generative adversarial framework for bounding confounded causal effects. In *Proceedings of the AAAI Conference on Artificial Intelligence*, volume 35, pages 12104–12112, 2021.

Yimin Huang and Marco Valtorta. Identifiability in causal bayesian networks: A sound and complete algorithm. In *Proceedings of the national conference on artificial intelligence*, volume 21, page 1149. Menlo Park, CA; Cambridge, MA; London; AAAI Press; MIT Press; 1999, 2006.

Yuanhanqing Huang and Jianghai Hu. A bandit learning method for continuous games under feedback delays with residual pseudo-gradient estimate. In *2023 62nd IEEE Conference on Decision and Control (CDC)*, pages 1207–1212. IEEE, 2023.

Eyke Hüllermeier and Willem Waegeman. Aleatoric and epistemic uncertainty in machine learning: An introduction to concepts and methods. *Machine learning*, 110(3):457–506, 2021.

Eyke Hüllermeier, Sébastien Destercke, and Mohammad Hossein Shaker. Quantification of credal uncertainty in machine learning: A critical analysis and empirical comparison. In *Uncertainty in Artificial Intelligence*, pages 548–557. PMLR, 2022.

Andrew Jesson, Sören Mindermann, Uri Shalit, and Yarin Gal. Identifying causal-effect inference failure with uncertainty-aware models. *Advances in Neural Information Processing Systems*, 33:11637–11649, 2020.

Wenlong Ji, Yihan Pan, Ruihao Zhu, and Lihua Lei. Multi-armed bandits with machine learning-generated surrogate rewards. *arXiv preprint arXiv:2506.16658*, 2025.

Ziwei Jiang and Murat Kocaoglu. Conditional common entropy for instrumental variable testing and partial identification. In *Forty-first International Conference on Machine Learning*, 2024.

Ziwei Jiang, Lai Wei, and Murat Kocaoglu. Approximate causal effect identification under weak confounding. In *International Conference on Machine Learning*, pages 15125–15143. PMLR, 2023.

Yonghan Jung, Shiva Kasiviswanathan, Jin Tian, Dominik Janzing, Patrick Blöbaum, and Elias Bareinboim. On measuring causal contributions via do-interventions. In *International Conference on Machine Learning*, pages 10476–10501. PMLR, 2022.

Nathan Kallus and Angela Zhou. Confounding-robust policy improvement. *Advances in neural information processing systems*, 31, 2018.

Murat Kocaoglu, Christopher Snyder, Alexandros G Dimakis, and Sriram Vishwanath. Causalgan: Learning causal implicit generative models with adversarial training. In *International Conference on Learning Representations*, 2018.

Ang Li and Judea Pearl. Bounds on causal effects and application to high dimensional data. In *Proceedings of the AAAI Conference on Artificial Intelligence*, volume 36, pages 5773–5780, 2022.

Ang Li, Scott Mueller, and Judea Pearl. Epsilon-identifiability of causal quantities. *arXiv preprint arXiv:2301.12022*, 2023.

Myrl G Marmarelis, Greg Ver Steeg, Aram Galstyan, and Fred Morstatter. Ensembled prediction intervals for causal outcomes under hidden confounding. In *Causal Learning and Reasoning*, pages 18–40. PMLR, 2024.

Valentyn Melnychuk, Stefan Feuerriegel, and Mihaela van der Schaar. Quantifying aleatoric uncertainty of the treatment effect: a novel orthogonal learner. *Advances in Neural Information Processing Systems*, 37: 105039–105089, 2024.

Leland Gerson Neuberg. Causality: models, reasoning, and inference, by judea pearl, cambridge university press, 2000. *Econometric Theory*, 19(4):675–685, 2003.

J. Pearl. *Causality*. Cambridge University Press, 2009. ISBN 9781139643986. URL <https://books.google.com/books?id=LLkhAwAAQBAJ>.

Judea Pearl. Causal diagrams for empirical research. *Biometrika*, 82(4):669–688, 1995.

Judea Pearl. On the testability of causal models with latent and instrumental variables. *arXiv preprint arXiv:1302.4976*, 2013.

Md Musfiqur Rahman and Murat Kocaoglu. Modular learning of deep causal generative models for high-dimensional causal inference. In *Forty-first International Conference on Machine Learning*, 2024. URL <https://openreview.net/forum?id=b0hzU7NpTB>.

Md Musfiqur Rahman, Matt Jordan, and Murat Kocaoglu. Conditional generative models are sufficient to sample from any causal effect estimand. *arXiv preprint arXiv:2402.07419*, 2024.

Murat Sensoy, Lance Kaplan, and Melih Kandemir. Evidential deep learning to quantify classification uncertainty. *Advances in neural information processing systems*, 31, 2018.

Amit Sharma and Emre Kiciman. Dowhy: An end-to-end library for causal inference. *arXiv preprint arXiv:2011.04216*, 2020.

Ilya Shpitser and Judea Pearl. Complete identification methods for the causal hierarchy. *Journal of Machine Learning Research*, 9:1941–1979, 2008.

Jin Tian. *Studies in causal reasoning and learning*. University of California, Los Angeles, 2002.

Jin Tian and Judea Pearl. Probabilities of causation: Bounds and identification. *Annals of Mathematics and Artificial Intelligence*, 28(1):287–313, 2000.

Jin Tian and Judea Pearl. A general identification condition for causal effects. In *Aaai/iaai*, pages 567–573, 2002.

Lai Wei, Muhammad Qasim Elahi, Mahsa Ghasemi, and Murat Kocaoglu. Approximate allocation matching for structural causal bandits with unobserved confounders. *Advances in Neural Information Processing Systems*, 36:68810–68832, 2023.

Kevin Xia, Kai-Zhan Lee, Yoshua Bengio, and Elias Bareinboim. The causal-neural connection: Expressiveness, learnability, and inference. *Advances in Neural Information Processing Systems*, 34:10823–10836, 2021.

Kevin Xia, Yushu Pan, and Elias Bareinboim. Neural causal models for counterfactual identification and estimation. *arXiv preprint arXiv:2210.00035*, 2022.

Mengyue Yang, Furui Liu, Zhitang Chen, Xinwei Shen, Jianye Hao, and Jun Wang. Causalvae: Disentangled representation learning via neural structural causal models. In *Proceedings of the IEEE/CVF conference on computer vision and pattern recognition*, pages 9593–9602, 2021.

Junzhe Zhang and Elias Bareinboim. Bounding causal effects on continuous outcome. In *Proceedings of the AAAI Conference on Artificial Intelligence*, volume 35, pages 12207–12215, 2021.

Zhiheng Zhang. Tight partial identification of causal effects with marginal distribution of unmeasured confounders. In *Forty-first International Conference on Machine Learning*, 2024.

## A Limitations and Future Works

A limitation of our methodology is the utilization of the epsilon-net to solve the challenging min-max and max-min problems required for performing this decomposition. Furthermore, neural network optimization may be imperfect in practice, giving smaller bounds than the true ones. In our future work, we aim to improve the min-max optimization and reduce the complexity of the  $\epsilon$ -net.

## B Related Work

**Partial Identification of Causal Effect.** When the causal effect is not identifiable from observational data, one can identify a set of causal effects from the SCMs that are compatible with the observational data. For the discrete variables, Balke and Pearl (1994, 2022) proposed a method using response variables to partition the latent variable into finite states and estimate the bounds of causal queries. Tian and Pearl (2000) used the response variable to get bounds of counterfactual queries from observational and interventional data. Many works focus on getting narrower bounds by utilizing additional information from the graph. Balke and Pearl (1997) obtained tighter bounds with instrumental variables. Duarte et al. (2024) proposed an automated method to derive bounds for causal queries in arbitrary graphs.

Another line of work tries to obtain narrower bounds of causal effect utilizing information from the unobserved confounders. Li and Pearl (2022) proposed using nonlinear programming to get bounds when the latent confounder is partially observed. Jiang et al. (2023) proposed a convex programming formulation to get tighter bounds of the causal effect when the entropy of the latent confounder is known. Li et al. (2023) derived bounds in closed form when the marginal distribution of the latent confounders is known. Zhang (2024) proposed a method that finds the tight identifiable region of causal effect given the marginal distribution of latent confounders.

**Causal Inference with Neural Models.** Many researchers have explored the use of neural networks in causal inference. Kocaoglu et al. (2018) introduced CausalGAN that produces interventional images with a GAN trained with image data. Yang et al. (2021) proposed CausalVAE to learn the causally related representations from the data. Xia et al. (2021, 2022) proposed neural causal models that find the causal and counterfactual queries by maximizing and minimizing the query under the semi-Markovian setting. Chao et al. (2023) proposed a diffusion-based approach to model the causal and counterfactual queries. Rahman and Kocaoglu (2024) proposed a modularized training algorithm to train a causal generative model with latent confounders for high-dimensional variables. Rahman et al. (2024) proposed a recursive algorithm that uses a set of conditional generative models to sample from any identifiable interventional distributions.

**Uncertainty Quantification.** Uncertainty quantification is a crucial problem in deep learning (Gal et al., 2016), especially in applications where reliable prediction is essential. Hora (1996) introduced the notion of aleatoric and epistemic to distinguish uncertainties for the risk models in applications such as decision making. Abellán et al. (2006) defined the total uncertainty based on the Shannon entropy of a credal set. Sensoy et al. (2018) quantified the epistemic uncertainty of the classification model with the Dirichlet prior. In general, the uncertainty is assumed to have an additive representation between the total uncertainty (TU), epistemic uncertainty (EU), and aleatoric uncertainty (AU), and it is generally hard to disentangle the EU and AU (Hüllermeier and Waegeman, 2021; Hüllermeier et al., 2022). Melnychuk et al. (2024) proposed a method for quantifying aleatoric uncertainty in individualized treatment effects by deriving sharp bounds on the conditional distributions of the treatment effect. Marmarelis et al. (2024) introduced an approach for constructing causal effect intervals with hidden confounding. Jiang and Kocaoglu (2024) proposed using entropy as a sensitivity parameter to obtain bounds in the IV graph with assumption violations.

**Decision Making.** Decision-making is highly related to the bandit problem, which aims to find the action that optimizes the rewards (Cho et al., 2024; Huang and Hu, 2023; Ji et al., 2025). In the context of causal inference, although the causal effect is closely related to the decision-making problem, Fernández-Loría and Provost (2022) suggested that they are not exactly equivalent, where the main distinction is their estimand of interest. Wei et al. (2023) proposed an algorithm that utilizes the causal graph to balance exploration and exploitation in sequential decision-making problems with latent confounders. Kallus and Zhou (2018) studied the decision-making problem with observational data with the presence of latent confounders. They showed that with a well-specified uncertainty set, the proposed robust policy learning is no worse than the baseline. Jesson et al. (2020) introduced a method to assess the uncertainty in the neural network model,

and demonstrated that the proposed method is able to handle the positivity violation. Sensitivity analysis is also closely related to the uncertainty quantification in causal inference. Frauen et al. (2023) proposed a neural framework for sensitivity analysis that is compatible with a large class of existing sensitivity models. Jesson et al. (2020) studied the decision-making problem under the non-overlapping situation. Frauen et al. (2025) propose a optimal decision-making approach based on two-stage CATE estimators.

## C Additional Discussion on Causal Effect Bounds

### C.1 Backdoor Example

For example, let us consider the backdoor graph example as shown in the top row of Figure 1. Let  $\hat{P}(y|x, z_i)$  and  $\hat{P}(z)$  be the empirical estimation from the data and  $l_i^y$  and  $u_i^y$  be the confidence intervals of the conditional probabilities  $\hat{P}(y|x, z_i)$ . Similarly,  $l_i^z$  and  $u_i^z$  are the confidence intervals of the conditional probabilities  $\hat{P}(z_i)$ . The for  $\hat{P}$  in the confidence set described by the above constraint, the maximum  $P(y|do(x))$  can be estimated by the following (left):

$$\begin{aligned} \max P(y|do(x)) &= \sum_i \hat{P}(y|x, z_i) \hat{P}(z_i) & \max P(y|do(x)) &= \sum_i u_i^y \hat{P}(z_i) \\ \text{s.t.} \quad \hat{P}(y|x, z_i) &\in [l_i^y, u_i^y]; \forall_i & \Rightarrow & \\ \hat{P}(z_i) &\in [l_i^z, u_i^z]; \forall_i & \text{s.t.} \quad \hat{P}(z_i) &\in [l_i^z, u_i^z]; \forall_i \\ \sum_i \hat{P}(z_i) &= 1 & \sum_i \hat{P}(z_i) &= 1 \end{aligned}$$

The objective function in the above optimization is a quadratic function, which could be nontrivial to solve. But in this case, since the  $a_i \in [l_i^y, u_i^y]$  are the only constraints for  $a_i$ , and the objective function is an affine function of  $a_i$ , the maximum is attained at the boundary when  $a_i = u_i^y \quad \forall i$ . The optimal solution of the above optimization problem can be found by the equivalent problem at the right, which can be solved through linear programming.

For intuitive discussion of our algorithm we introduce the following concept.

**Definition 11** (Solid region).  $[\bar{L}, \bar{U}]$ : *Intersection of all [min, max] causal effect intervals induced by each empirical distribution  $\hat{P}$  in the confidence interval.*

**Definition 12** (Inner ate bound:  $[\bar{U}_{ate}, \bar{U}_{ate}]$ , Outer ate band  $[\underline{L}_{ate}, \bar{L}_{ate}] \cup [\bar{U}_{ate}, \bar{U}_{ate}]$ ). *Given a confidence set  $\mathcal{C}$ , we access the sample and non-id uncertainty regions by estimating four quantities for ATE as following.*

$$\begin{aligned} \bar{U}_{ate} &:= \max_{P \in \mathcal{C}(\hat{P})} \max_{S \in \mathcal{S}_P} ATE(x(S)) \\ \underline{U}_{ate} &:= \min_{P \in \mathcal{C}(\hat{P})} \max_{S \in \mathcal{S}_P} ATE(x(S)) \\ \bar{L}_{ate} &:= \max_{P \in \mathcal{C}(\hat{P})} \min_{S \in \mathcal{S}_P} ATE(x(S)) \\ \underline{L}_{ate} &:= \min_{P \in \mathcal{C}(\hat{P})} \min_{S \in \mathcal{S}_P} ATE(x(S)), \end{aligned} \tag{2}$$

### C.2 Effect of sample size on individual action interval

Suppose, we have are given  $N$  samples from the true distribution  $P(\cdot)$  resulting in an empirical distribution  $\hat{P}$ . From the samples, we can construct confidence regions  $\mathcal{C}_{P(\cdot)}$ . Any distribution  $P_\epsilon \in \mathcal{C}_{P(\cdot)}$  with  $d(P_\epsilon, \hat{P}) < \epsilon$  can be the true distribution. We maximize the causal effect while keeping the empirical distribution in this region. Suppose all the empirical distributions  $P_\epsilon \in \mathcal{C}$  provides us a set of max causal effects  $M_{P(y|do(x))}$ .

Now, suppose, we have less samples than  $N$ . Less samples will make a larger confidence region  $\mathcal{C}^L$  allowing more empirical distributions as potential candidate to be the true distribution. As a result we will have a new set of max causal effect  $M'_{P(y|do(x))}$  for the distributions  $P_\epsilon \in \mathcal{C}^L \setminus \mathcal{C}$ . Now,  $\bar{U} = \max(M_{P(y|do(x))}, M'_{P(y|do(x))}) \geq \max(M_{P(y|do(x))})$  and  $\underline{U} = \min(M_{P(y|do(x))}, M'_{P(y|do(x))}) \leq \min(M_{P(y|do(x))})$ . Thus, when we have low sample

size, the bound  $[\underline{U}, \bar{U}]$  extends. Similarly, the bound  $[\underline{L}, \bar{L}]$  also extends when we have low sample size. As the above two bounds extend, the bound  $[\bar{L}, \underline{U}]$  shrinks.

Now, suppose, we have more samples than  $N$ . More samples will make a smaller confidence region  $\mathcal{C}^S$  allowing less empirical distributions as potential candidate to be the true distribution. As a result we will have a new set of max causal effect  $M'_{P(y|do(x))}$ . for the distributions  $P_\epsilon \in \mathcal{C}^S$ . Now,  $\bar{U} = \max(M'_{P(y|do(x))}) \leq \max(M_{P(y|do(x))})$  and  $\underline{U} = \min(M'_{P(y|do(x))}) \geq \min(M_{P(y|do(x))})$ . Thus, when we have high sample size, the bound  $[\underline{U}, \bar{U}]$  shrinks. Similarly, the bound  $[\underline{L}, \bar{L}]$  also shrinks when we have low sample size. As the above two bounds shrink, the bound  $[\bar{L}, \underline{U}]$  extends.

The consequence of sample size can also be visualized as imagining  $\max p(y|do(x))$  as an estimand. With finite samples, there is a confidence interval below and above it. which is  $\min \max p(y|do(x))$  and  $\max \max p(y|do(x))$ . With fewer samples, this confidence interval gets wider. So the  $\min \max p(y|do(x))$  will be smaller. Similarly, the  $\max \min p(y|do(x))$  will be larger.

### C.3 Derivation of Confidence Intervals

**Calculate Confidence Intervals** We calculate the confidence interval for any conditional distribution  $P(v_i|v^{\pi_i-1})$  as below:

First, we need to obtain the empirical estimators  $\hat{P}(v_i = 1|v^{\pi_i-1})$  for the binary variables from the training data.  $\hat{P}_n(v_i = 1|v^{\pi_i-1}) = \frac{1}{m} \sum_{k=1}^m \mathbb{1}(v_i^k(v^{\pi_i-1}) = 1)$

Now, let  $n = \text{count}(D[v^{\pi_i-1}])$ . Then according to Hoeffding inequality:

$$\begin{aligned}
 \Pr(|\hat{P} - P| \geq \epsilon) &\leq 2e^{-2n\epsilon^2} \\
 \alpha &= 2e^{-2n\epsilon^2} \\
 \alpha/2 &= e^{-2n\epsilon^2} \\
 \ln(2/\alpha) &= 2n\epsilon^2 \\
 \frac{\ln(2/\alpha)}{2n} &= \epsilon^2 \\
 \epsilon &= \sqrt{\frac{\ln(2/\alpha)}{2n}}
 \end{aligned} \tag{3}$$

Thus, the confidence interval for our empirical estimators are:

$$\begin{aligned}
 \mathcal{C}_{P(v_i=1|v^{\pi_i-1})} &:= \left( \hat{P}_n(v_i = 1|v^{\pi_i-1}) - \sqrt{\frac{\ln(2/\alpha)}{2n}}, \hat{P}_n(v_i = 1|v^{\pi_i-1}) + \sqrt{\frac{\ln(2/\alpha)}{2n}} \right) \\
 P(v_i = 1|v^{\pi_i-1}) &\in \mathcal{C}_{P(v_i=1|v^{\pi_i-1})} \quad \text{with probability greater than } 1 - \alpha
 \end{aligned}$$

## D Theoretical Analysis

**Assumption 1.** *We assume the variables are discrete.*

In the binary case, confidence intervals are defined over single conditional probabilities, which simplifies the exploration within the  $\epsilon$ -ball. For a non-binary variable  $X$  with  $|\mathcal{X}|$  states, there will be  $|\mathcal{X}| - 1$  confidence intervals due to the simplex constraint. Constructing valid distributions from these confidence intervals becomes a difficult constrained optimization problem.

**Assumption 2.** *The structural causal model is Semi-Markovian.*

**Assumption 3.** *We have access to the acyclic directed mixed graph (ADMG).*

**Lemma 1.** *Let  $L_i, U_i$  be the upper bound and lower bound of  $\text{ATE}(x_0, x_i)$ . Action  $x_0$  is the best action if and only if  $L_i \geq 0 \forall i \neq 1$ .*

*Proof.*  $\implies$  is clear from the definition.

$\impliedby$  : Suppose for the sake of contradiction that there exists some SCM such that  $\text{ATE}(x_0, x_j) < 0$ . But this contradicts the assumption that  $L_i \geq 0 \forall i \neq 1$ .  $\square$

**Lemma 2.** *If there exists any  $x_i$  such that  $U_i > 0$  and  $L_i < 0$ , then both  $x_0$  and  $x_i$  cannot be the best action.*

*Proof.* If there exists any  $x_i$  such that  $U_i > 0$  and  $L_i < 0$ , that means there exist two SCM  $S1, S2$  such that  $\text{ATE}(x_0, x_i) > 0$  in  $S1$ , and  $\text{ATE}(x_0, x_i) < 0$  in  $S2$ . So both  $x_0$  and  $x_i$  cannot be determined to be the best action.  $\square$

## D.1 Proof of Theorem 2

**Theorem 8** (Main Paper Theorem 2). *Let  $f(P, G)$  be the estimand of some identifiable causal effect of interest for a causal graph  $G$  (possibly with latents), and the observational distribution  $P$ . Let  $\mathcal{P}$  be any connected set of observational distributions that contains  $P$ . Let  $a = \min_{P \in \mathcal{P}} f(P, G), b = \max_{P \in \mathcal{P}} f(P, G)$ . Then  $f : \mathcal{P} \rightarrow [a, b]$  is surjective.*

*Proof.* Consider any connected set of observed distributions  $\mathcal{P}$ . For any  $P \in \mathcal{P}$ , let  $\bar{P}$  be the distribution including the latent variables  $U$ , such that  $\sum_U \bar{P} = P$ . Assume the causal query is well defined, i.e.  $P(pa(y)) > 0$ .

Let  $\text{adj}(X, Y)$  be the set of variables that are the parents of  $Y$  but not descendants of  $X$ . Then

$$\begin{aligned} f(\bar{P}, G) &= P(y|do(x)) \\ &= \sum_{\text{adj}(X, Y)} \bar{P}(y|x, \text{adj}(X, Y)) \bar{P}(\text{adj}(X, Y)) \\ &= \frac{\sum_{v \notin \{x, y, \text{adj}(X, Y)\}} \bar{P}(v)}{\sum_{v \notin \{x, \text{adj}(X, Y)\}} \bar{P}(v)} \left( \sum_{v \notin \{\text{adj}(X, Y)\}} \bar{P}(v) \right). \end{aligned}$$

Since the causal effect is a rational function of  $\bar{P}$ , it is continuous when the denominator is strictly positive.

Define  $h_G(P)$  be the function that maps  $P \in \mathcal{P}$  to some causal effect in  $[0, 1]$  such that  $h_G(P) = f(\bar{P}, S) \forall \sum_u \bar{P} = P$ . Since the query is identifiable, the value of  $f(\bar{P}, S)$  is identical for all  $\{\bar{P} \mid \sum_U \bar{P} = P, P \in \mathcal{P}\}$ . So  $h_G$  is well defined.

Now for any open subset  $M \subseteq [0, 1]$ , since  $f$  is continuous, the preimage  $f^{-1}(M) \subseteq \{\bar{P} \mid \sum_U \bar{P} = P, P \in \mathcal{P}\}$  is open. Let  $g$  be the function mapping full joint distribution to observed distribution, i.e.,  $g : \bar{P} \mapsto P$ . By our construction, for any  $P \in \mathcal{P}$ ,  $g : f^{-1}(M) \rightarrow P$  is a linear surjective function. By the open mapping theorem, since  $f^{-1}(M)$  is open, the image of  $g$  is open. Therefore, the function  $h_G$  is continuous. And since the query is identifiable,  $f(P, G) = h_G(P) \forall P \in \mathcal{P}$ .

So by the generalized intermediate value theorem, the image of  $f(\mathcal{P}, G)$  is connected. Since the image is a subset of  $[0, 1]$ , it is an interval that contains  $[a, b]$ .  $\square$

## D.2 Proof of Theorem 3

**Theorem 9** (Main Paper Theorem 3). *Let  $f(p, S)$  be the estimand of some non-identifiable causal effect of interest for some causal graph, and the observational distribution  $p$ . Let  $\mathcal{S}$  be the set of the SCM such that  $P_{\text{obs}}(S) = p$ . Let  $a = \min_{S \in \mathcal{S}} f(p, S), b = \max_{S \in \mathcal{S}} f(p, S)$ . Then  $f|_p : \mathcal{S} \rightarrow [a, b]$  is surjective.*

*Proof.* Suppose the causal query of interest is  $P(y|do(x))$ . Consider the graph  $G$  that includes both observed and unobserved latent variables. Let  $\mathcal{P}$  be the set of distributions over the graph  $G$ . For each  $\bar{P} \in \mathcal{P}$ , let the set of  $\bar{P}$  denote the underlying SCM, i.e.  $S = \bar{P}$  for some  $\bar{P} \in \mathcal{P}$ . Assume the causal query is well defined, i.e.  $P(pa(y)) > 0$ . Then

$$f(p, S) = P(y|do(x)) = \sum_{pa(y)} \bar{P}(y|pa(y)) \bar{P}(pa(y)) = \frac{\sum_{v \notin \{x, y, pa(y)\}} \bar{P}(v)}{\sum_{v \notin \{x, pa(y)\}} \bar{P}(v)} \left( \sum_{v \notin \{pa(y)\}} \bar{P}(v) \right).$$

So the causal effect is a rational function of the full distribution over  $G$ . Since the causal query is well defined, the denominator is strictly positive. Thus  $f(p, S)$  is continuous over all  $\bar{P} \in \mathcal{P}$ . For each  $\bar{P} \in \mathcal{P}$ , the

only set of constraints are in form of  $\sum_{u \in U} \bar{P}(v, u) = P(v)$ . The set  $\mathcal{P}$  is connected. Therefore, the image of  $f(p, \cdot)$  is connected, and thus it is an interval. Since there is exist  $f(p, S) = a$  and  $f(p, S) = b$ , and the image of  $f(p, S)$  is connected,  $[a, b] \subseteq f(p, \mathcal{S})$ . so the map  $f(p, \cdot)$  is surjective.  $\square$

### D.3 Proof of Proposition 1

**Proposition 5** (Main Paper Proposition 1). *The nonID uncertainty of the causal decision making problem cannot be reduced by increasing the number of samples in the data.*

$$\begin{aligned}\bar{U}_x &:= \max_{P \in \mathcal{C}(\hat{P})} \max_{S \in \{S \text{ an SCM} | P_{\text{obs}}(S) = P, S \models G\}} P_S(Y | \text{do}(X = x)) \\ \underline{U}_x &:= \min_{P \in \mathcal{C}(\hat{P})} \max_{S \in \{S \text{ an SCM} | P_{\text{obs}}(S) = P, S \models G\}} P_S(Y | \text{do}(X = x)) \\ \bar{L}_x &:= \max_{P \in \mathcal{C}(\hat{P})} \min_{S \in \{S \text{ an SCM} | P_{\text{obs}}(S) = P, S \models G\}} P_S(Y | \text{do}(X = x)) \\ \underline{L}_x &:= \min_{P \in \mathcal{C}(\hat{P})} \min_{S \in \{S \text{ an SCM} | P_{\text{obs}}(S) = P, S \models G\}} P_S(Y | \text{do}(X = x)),\end{aligned}\tag{4}$$

Since the confidence set gets strictly smaller as more samples are added to the dataset, for each epsilon ball, the search space of joint distributions is strictly smaller. As shown in Theorem 3, the inner region  $[\bar{L}_x, \underline{U}_x]$  is the intersection of all intervals  $\mathcal{I}_P$ . As the search space of joint distribution is smaller, there are less distributions to search over, and therefore less number of  $\mathcal{I}_P$ . The size of  $\mathcal{C}(\hat{P})$  decreases, the  $\underline{U}_x$  will increase as more samples are collected. Similarly,  $\bar{L}_x$  will decrease as the number of samples increases. Hence, the nonID uncertainty represented by  $[\bar{L}_x, \underline{U}_x]$  will not decrease as the number of samples increases.  $\square$

### D.4 Proof of Proposition 2

**Proposition 6** (Main Paper Proposition 2). *There exists SCMs  $S \in \mathcal{S}_P$  where the sample uncertainty of the causal decision making problem can be reduced by increasing the number of samples in the data.*

*Proof.* By the definition, the sample uncertainty are the intervals  $[\underline{U}_x, \bar{U}_x]$  and  $[\underline{L}_x, \bar{L}_x]$ . As the number of samples increases, the epsilon ball that is searched over is strictly smaller. Therefore the size of  $\mathcal{C}(\hat{P})$  decrease, and the  $\bar{U}_x$  will decrease as  $\underline{U}_x$  will increase, hence the interval  $[\underline{U}_x, \bar{U}_x]$  becomes narrower. Similarly for  $[\underline{L}_x, \bar{L}_x]$ .  $\square$

**Theorem 10.** [Main Paper Theorem 5] *For a causal decision making problem, let  $(\bar{U}_{x_0}, \underline{U}_{x_0}, \bar{L}_{x_0}, \underline{L}_{x_0})$ , and  $(\bar{U}_{x_1}, \underline{U}_{x_1}, \bar{L}_{x_1}, \underline{L}_{x_1})$  be estimated from the data. The decision is unambiguous if  $\underline{L}_{x_1} > \bar{U}_{x_0}$  or  $\underline{L}_{x_0} > \bar{U}_{x_1}$ . The decision cannot be improved with more data if  $\bar{L}_{x_1} < \underline{U}_{x_0} < \underline{U}_{x_1}$  or  $\bar{L}_{x_1} < \bar{L}_{x_0} < \underline{U}_{x_1}$ .*

*Proof.* Without loss of generality, assuming  $\underline{L}_{x_1} > \bar{U}_{x_0}$ , for all SCMs that are compatible with the observational data, we have  $P(y | \text{do}(x_1)) \geq \underline{L}_{x_1}$  and  $P(y | \text{do}(x_0)) \leq \bar{U}_{x_0}$ . By the definition, the decision is unambiguous.

For the second claim, without loss of generality, assume  $\bar{L}_{x_1} < \underline{U}_{x_0} < \underline{U}_{x_1}$ . As the number of samples goes to infinity,  $\hat{P} \rightarrow P$  and therefore both  $\bar{U}_{x_1}, \underline{U}_{x_1}$  converge to a point, denotes  $U_{x_1}$ . Similarly, both  $\underline{L}_{x_1}, \bar{L}_{x_1}$  converge to a point denotes  $L_{x_1}$ . In addition,  $\underline{U}_{x_1} \leq U_{x_1} \leq \bar{U}_{x_1}$  and  $\underline{L}_{x_1} \leq L_{x_1} \leq \bar{L}_{x_1}$ . So the nonID uncertainty converges to  $[L_{x_1}, U_{x_1}]$  as the number of samples goes to infinity. By proposition D.3, the nonID cannot be improved by increasing the number of samples in the data. So  $\underline{U}_{x_1} \leq U_{x_1}$  and  $\bar{L}_{x_1} \geq L_{x_1}$ . Since the bounds  $[L_{x_1}, U_{x_1}]$  are achievable, there exists SCM  $S_1$  and  $S_2$  such that for  $S_1$ ,  $P(y_1 | \text{do}(x_0)) = \underline{U}_{x_0}$ ,  $P(y_1 | \text{do}(x_1)) = \bar{L}_{x_1}$ ; and for  $S_2$ ,  $P(y_1 | \text{do}(x_0)) = \underline{U}_{x_0}$ ,  $P(y_1 | \text{do}(x_1)) = \underline{U}_{x_1}$ . By the definition, the decision is ambiguous. And by proposition D.3, the interval  $[\bar{L}_{x_1}, \underline{U}_{x_1}]$  cannot be reduced with additional data samples.  $\square$

The following lemma applies even with unobserved confounding between  $X, Y$ .

**Lemma 3.** Consider the causal graph with binary  $X, Y, Z$  where  $Z$  is an observed confounder with observational distribution  $P(X, Y, Z)$ . Consider another joint distribution  $P'(X, Y, Z)$ . If  $TVD(P(X, Y|Z = z), P'(X, Y|Z = z)) < \epsilon$  and  $TVD(P(Z), P'(Z)) < \epsilon$  then  $|f(p) - f(p')| \leq 3\epsilon$  where  $f(p) = \max_{\{S|P_{obs}(S)=p\}} p_S(y|do(x))$ .

*Proof.* Consider the bow-backdoor graph with binary variables  $X, Y, Z$  where  $Z$  is a confounder. Define the response variables  $R_y, R_x$  as follows.

$R_x$	$z_0$	$z_1$
0	$y_0$	$y_0$
1	$y_0$	$y_1$
2	$y_1$	$y_0$
3	$y_1$	$y_1$

Table 1: Response function  $R_x$

$R_y$	$z_0, x_0$	$z_0, x_1$	$z_1, x_0$	$z_1, x_1$
0	$y_0$	$y_0$	$y_0$	$y_0$
1	$y_0$	$y_0$	$y_0$	$y_1$
2	$y_0$	$y_0$	$y_1$	$y_0$
3	$y_0$	$y_0$	$y_1$	$y_1$
4	$y_0$	$y_1$	$y_0$	$y_0$
5	$y_0$	$y_1$	$y_0$	$y_1$
6	$y_0$	$y_1$	$y_1$	$y_0$
7	$y_0$	$y_1$	$y_1$	$y_1$
8	$y_1$	$y_0$	$y_0$	$y_0$
9	$y_1$	$y_0$	$y_0$	$y_1$
10	$y_1$	$y_0$	$y_1$	$y_0$
11	$y_1$	$y_0$	$y_1$	$y_1$
12	$y_1$	$y_1$	$y_0$	$y_0$
13	$y_1$	$y_1$	$y_0$	$y_1$
14	$y_1$	$y_1$	$y_1$	$y_0$
15	$y_1$	$y_1$	$y_1$	$y_1$

Table 2: Response function  $R_y$

Let  $f(p) = \max p(y_0|do(x_0))$  then we can express  $f(p)$  with response variables as following

$$f(p) = \sum_j \left( \left( \sum_{i=0}^7 q_{i,j} p(z_0) \right) + \left( \sum_{i=\{0,1,4,5,8,9,12,13\}} q_{i,j} p(z_1) \right) \right) \quad (5)$$

where  $q_{i,j} = p(R_x = i, R_y = j)$

$$\mathbf{A} = \begin{bmatrix} 1 & q_{0,0} \\ 1 & q_{0,1} \\ 1 & q_{0,4} \\ 1 & q_{0,5} \\ p(z_0) & q_{0,2} \\ p(z_0) & q_{0,3} \\ p(z_0) & q_{0,6} \\ p(z_0) & q_{0,7} \\ p(z_1) & q_{0,8} \\ p(z_1) & q_{0,9} \\ p(z_1) & q_{0,12} \\ p(z_1) & q_{0,13} \\ 1 & q_{1,0} \\ \vdots & \vdots \end{bmatrix}, \quad \mathbf{v} = \begin{bmatrix} q_{0,0} \\ q_{0,1} \\ q_{0,4} \\ q_{0,5} \\ q_{0,2} \\ q_{0,3} \\ q_{0,6} \\ q_{0,7} \\ q_{0,8} \\ q_{0,9} \\ q_{0,12} \\ q_{0,13} \\ q_{1,0} \\ \vdots \end{bmatrix}$$

$$\mathbf{v}_{z_0} = \begin{bmatrix} q_{0,0} \\ q_{0,1} \\ q_{0,2} \\ q_{0,3} \\ q_{0,4} \\ q_{0,5} \\ q_{0,6} \\ q_{0,7} \\ q_{1,0} \\ \vdots \end{bmatrix}, \quad \mathbf{v}_{z_1} = \begin{bmatrix} q_{0,0} \\ q_{0,1} \\ q_{0,4} \\ q_{0,5} \\ q_{0,8} \\ q_{0,9} \\ q_{0,12} \\ q_{0,13} \\ q_{1,0} \\ \vdots \end{bmatrix}$$

The domain of  $\mathbf{x}$  is defined by the following constraints

$$\begin{aligned} p(y_0, x_0 | z_0) &= q_{0,0} + q_{0,1} + q_{0,2} + q_{0,3} + q_{0,4} + q_{0,5} + q_{0,6} + q_{0,7} \\ &\quad + q_{1,0} + q_{1,1} + q_{1,2} + q_{1,3} + q_{1,4} + q_{1,5} + q_{1,6} + q_{1,7} \\ p(y_0, x_0 | z_1) &= q_{0,0} + q_{0,1} + q_{0,4} + q_{0,5} + q_{0,8} + q_{0,9} + q_{0,12} + q_{0,13} \\ &\quad + q_{2,0} + q_{2,1} + q_{2,4} + q_{2,5} + q_{2,8} + q_{2,9} + q_{2,12} + q_{2,13} \\ &\quad \dots \\ p(y_1, x_1 | z_1) &= \dots \end{aligned}$$

Assume  $TVD(P(X, Y | z), P'(X, Y | z)) \leq \epsilon$  and  $TVD(P(Z), P'(Z)) \leq \epsilon$  for each  $z$ .

Let  $k_{xyz} = \{i, j | \sum q_{i,j} = p(x, y | z)\}$ . From the construction, for each  $z$ ,  $k_{xyz}$  are non-overlap for each  $Z = z$ , and  $\sum_{xy} k_{xyz} = 1$ .

Since  $TVD(P(Z), P'(Z)) \leq \epsilon$ ,  $|p(z) - p'(z)| \leq \epsilon$  for all  $z$ .

Let  $S_z = \{x, y, z | k_{xyz} \cap \mathbf{v}_z \neq \emptyset\}$  Then we have

$$\begin{aligned} \frac{1}{2} \sum_{x, y, z \in S_z} |(p(x, y | z) - p'(x, y | z))| &\leq \frac{\epsilon}{2} \\ \sum_{x, y, z \in S_z} \left| \sum_{i, j \in k_{xyz}} (q_{i,j} - q'_{i,j}) \right| &\leq \epsilon \\ |\sum \mathbf{v}_z - \sum \mathbf{v}'_z| &\leq \epsilon \end{aligned} \tag{6}$$

Hence

$$\begin{aligned}
|f(p) - f(p')| &= \left| \left( p(z_0) \sum \mathbf{v}_{z_0} + p(z_1) \sum \mathbf{v}_{z_1} \right) - \left( p'(z_0) \sum \mathbf{v}'_{z_0} + p'(z_1) \sum \mathbf{v}'_{z_1} \right) \right| \\
&= \left| \left( p(z_0) \sum \mathbf{v}_{z_0} - p'(z_0) \sum \mathbf{v}'_{z_0} \right) + \left( p(z_1) \sum \mathbf{v}_{z_1} - p'(z_1) \sum \mathbf{v}'_{z_1} \right) \right| \\
&\leq \left| \left( p(z_0) \sum \mathbf{v}_{z_0} - p'(z_0) \sum \mathbf{v}'_{z_0} \right) \right| + \left| \left( p(z_1) \sum \mathbf{v}_{z_1} - p'(z_1) \sum \mathbf{v}'_{z_1} \right) \right| \\
&= \left| \left( p(z_0) \sum \mathbf{v}_{z_0} - p(z_0) \sum \mathbf{v}'_{z_0} + p(z_0) \sum \mathbf{v}'_{z_0} - p'(z_0) \sum \mathbf{v}'_{z_0} \right) \right| \\
&\quad + \left| \left( p(z_1) \sum \mathbf{v}_{z_1} - p(z_1) \sum \mathbf{v}'_{z_1} + p(z_1) \sum \mathbf{v}'_{z_1} - p'(z_1) \sum \mathbf{v}'_{z_1} \right) \right| \\
&= \left| p(z_0) \left( \sum \mathbf{v}_{z_0} - \sum \mathbf{v}'_{z_0} \right) + \sum v'_{z_0} (p(z_0) - p'(z_0)) \right| \\
&\quad + \left| p(z_1) \left( \sum \mathbf{v}_{z_1} - \sum \mathbf{v}'_{z_1} \right) + \sum v'_{z_1} (p(z_1) - p'(z_1)) \right| \\
&\leq p(z_0) \epsilon + \sum v'_{z_0} \epsilon + p(z_1) \epsilon + \sum v'_{z_1} \epsilon \\
&\leq 3\epsilon
\end{aligned} \tag{7}$$

□

**Corollary 3.** For binary variables  $X, Y$  with a binary confounder  $Z$  and latent confounders. The  $\underline{U}_x$  and  $\bar{L}_x$  estimated from our algorithm are within  $3\epsilon$  distance from the true values.

*Proof.* Let  $\underline{U}_x$  denote the true  $\min \max P(y|do(x))$  and  $\hat{U}_x$  denote the estimated value of our algorithm. Suppose for the sake of contradiction that  $|\hat{U}_x - \underline{U}_x| > 3\epsilon$ . By Lemma 1, the observed distributions that are compatible with  $\underline{U}_x$  and  $\hat{U}_x$  do not belong to the same ball with  $\epsilon$  distance. Let  $B$  be the ball that contains the observed distribution that is compatible with  $\underline{U}_x$ , and  $U_x$  be the maximum value of  $P(y|do(x))$  with a compatible observational distribution inside  $B$ . By Lemma 1,  $|U - \underline{U}_x| \leq 3\epsilon$ . Since  $\underline{U}_x, \hat{U}_x, U$  are scalers and  $\underline{U}_x$  is the smallest  $\max P(y|do(x))$  over all observational distributions, we have  $U - \underline{U}_x \leq 3\epsilon$ ,  $\hat{U}_x - \underline{U}_x > 3\epsilon$ . And that implies  $\hat{U}_x > U$ , which contradicts the assumption that  $\hat{U}_x$  is the smallest  $\max P(y|do(x))$  among all epsilon balls. So we can conclude that  $|\hat{U}_x - \underline{U}_x| \leq 3\epsilon$  □

**Lemma 4.** For an observational distribution from IV graph  $P(X, Y, Z)$  where  $X, Y, Z$  are binary variables, there exist a SCM such that  $P(y_1|do(x_1))$  attains the upper bound and  $P(y_1|do(x_0))$  attains the lower bound.

*Proof.* Let  $R_x, R_y$  be the response variables for  $X, Y$ , and  $q_{ij} := P(R_x = i, R_y = j)$ . Then we have the following constraints from the observed data.

$$\begin{aligned}
P(y_0, x_0|z_0) &= q_{00} + q_{10} + q_{01} + q_{11} \\
P(y_0, x_1|z_0) &= q_{20} + q_{22} + q_{30} + q_{32} \\
P(y_1, x_0|z_0) &= q_{02} + q_{03} + q_{12} + q_{13} \\
P(y_1, x_1|z_0) &= q_{21} + q_{23} + q_{31} + q_{33} \\
P(y_0, x_0|z_1) &= q_{00} + q_{20} + q_{01} + q_{21} \\
P(y_0, x_1|z_1) &= q_{10} + q_{12} + q_{30} + q_{32} \\
P(y_1, x_0|z_1) &= q_{02} + q_{03} + q_{22} + q_{23} \\
P(y_1, x_1|z_1) &= q_{11} + q_{13} + q_{31} + q_{33}
\end{aligned}$$

$$\begin{aligned}
P(y_1|do(x_1)) &= \sum_{i=0}^3 q_{i1} + q_{i3} \\
P(y_1|do(x_0)) &= \sum_{i=0}^3 q_{i2} + q_{i3}
\end{aligned}$$

The goal is to show an SCM that obtains the minimum of  $P(y_1|do(x_0))$  and the maximum of  $P(y_1|do(x_1))$ . For the SCM minimize  $P(y_1|do(x_0))$ , the corresponding  $q_{ij}$  are minimized. Without loss of generality, assume  $P(y_1, x_0|z_1) > P(y_1, x_0|z_0)$ . The minimum of  $P(y_1|do(x_0))$  can be obtained by let  $q_{12}, q_{13}, q_{32}, q_{33}$  equal to zero (because the constraint  $P(y_1, x_0|z_1) = q_{02} + q_{03} + q_{22} + q_{23}$ , the terms  $q_{02}, q_{03}, q_{22}, q_{23}$  do not affect the value of  $P(y_1|do(x_0))$ ).

Similarly, for the maximum of  $P(y_1|do(x_1))$ , without loss of generality, assume  $P(y_0, x_1|z_1) > P(y_0, x_1|z_0)$ . To maximize  $P(y_1|do(x_1)) = \sum_{i=0}^3 q_{i1} + q_{i3}$ , let  $q_{01} + q_{21} = P(y_0, x_0|z_1)$ , and  $q_{03} + q_{23} = P(y_1, x_0|z_1)$  (due to the constraint  $P(y_1, x_1|z_1) = q_{11} + q_{13} + q_{31} + q_{33}$ , the terms  $q_{11}, q_{13}, q_{31}, q_{33}$  do not affect the value of  $P(y_1|do(x_1))$ ). This is equivalent to making  $q_{00}, q_{20}, q_{02}, q_{22}$  equal to zero.

Combining the two derivations above, any SCM with response variables such that  $q_{00}, q_{20}, q_{02}, q_{22}, q_{12}, q_{13}, q_{32}, q_{33}$  equals to zero would attains the maximum of  $P(y_1|do(x_1))$  and minimum of  $P(y_1|do(x_0))$ .  $\square$

## D.5 Proof of theorem 4

*Proof.* Let  $m_P = \min \mathcal{I}_P = \min_{S \in \{S \text{ an SCM} | P_{\text{obs}}(S)=P\}} P_S(Y|do(X=x))$  and  $\mathcal{M} = \{m_P | P \in \mathcal{C}\}$ . Then  $\min \bigcap_{P \in \mathcal{C}} \mathcal{I}_P = \max \mathcal{M} = \max \min_{S \in \{S \text{ an SCM} | P_{\text{obs}}(S)=P\}} P_S(Y|do(X=x)) = \overline{L}_{do(x)}$ .

By a symmetric argument, we can show that  $\max \bigcap_{P \in \mathcal{C}} \mathcal{I}_P = \max \min_{S \in \{S \text{ an SCM} | P_{\text{obs}}(S)=P\}} P_S(Y|do(X=x)) = \underline{U}_{do(x)}$ .  $\square$

## D.6 Proof of corollary 1

*Proof.* Since  $\bigcap_{P \in \mathcal{C}} \mathcal{I}_P = [\overline{L}_{do(x)}, \underline{U}_{do(x)}]$ , we only need to show that  $\bigcup_{P \in \mathcal{C}} \mathcal{I}_P = [\underline{L}_{do(x)}, \overline{U}_{do(x)}]$ . Let  $m_P = \min \mathcal{I}_P = \min_{S \in \{S \text{ an SCM} | P_{\text{obs}}(S)=P\}} P_S(Y|do(X=x))$  and  $\mathcal{M} = \{m_P | P \in \mathcal{C}\}$ . Then  $\min \bigcup_{P \in \mathcal{C}} \mathcal{I}_P = \min \mathcal{M} = \min \min_{S \in \{S \text{ an SCM} | P_{\text{obs}}(S)=P\}} P_S(Y|do(X=x)) = \underline{L}_{do(x)}$ . Similarly, by a symmetric argument, we have  $\max \bigcup_{P \in \mathcal{C}} \mathcal{I}_P = \overline{U}_{do(x)}$   $\square$

## D.7 Proof of theorem 6

*Proof.* Let  $m_P = \min \mathcal{I}_P = \min_{S \in \{S \text{ an SCM} | P_{\text{obs}}(S)=P\}} ATE(x)$  and  $\mathcal{M} = \{m_P | P \in \mathcal{C}\}$ . Then  $\min \bigcap_{P \in \mathcal{C}} \mathcal{I}_P = \max \mathcal{M} = \max \min_{S \in \{S \text{ an SCM} | P_{\text{obs}}(S)=P\}} ATE(x) = \overline{L}_{ate_x}$ .

By a symmetric argument, we can show that  $\max \bigcap_{P \in \mathcal{C}} \mathcal{I}_P = \max \min_{S \in \{S \text{ an SCM} | P_{\text{obs}}(S)=P\}} ATE(x) = \underline{U}_{ate_x}$ .  $\square$

## D.8 Proof of corollary 2

*Proof.* Since  $\bigcap_{P \in \mathcal{C}} \mathcal{I}_P = [\overline{L}_{ate_x}, \underline{U}_{ate_x}]$ , we only need to show that  $\bigcup_{P \in \mathcal{C}} \mathcal{I}_P = [\underline{L}_{ate_x}, \overline{U}_{ate_x}]$ . Let  $m_P = \min \mathcal{I}_P = \min_{S \in \{S \text{ an SCM} | P_{\text{obs}}(S)=P\}} ATE(x)$  and  $\mathcal{M} = \{m_P | P \in \mathcal{C}\}$ . Then  $\min \bigcup_{P \in \mathcal{C}} \mathcal{I}_P = \min \mathcal{M} = \min \min_{S \in \{S \text{ an SCM} | P_{\text{obs}}(S)=P\}} ATE(x) = \underline{L}_{ate_x}$ . Similarly, by a symmetric argument, we have  $\max \bigcup_{P \in \mathcal{C}} \mathcal{I}_P = \overline{U}_{ate_x}$   $\square$

## D.9 Proof of theorem 7

*Proof.* By the definition of  $ATE(x)$ , for a fixed SCM, an action  $x$  is the best action if  $ATE(x) \geq 0$ . For a fixed distribution  $P$ ,  $\mathcal{I}_P$  corresponds to the values of  $ATE(x)$  with the set of SCMs that is compatible with  $P$ , where each SCM corresponds to a unique value of  $ATE(x)$ . And if  $ATE(x) \geq 0$  for some  $x$ , the action  $x$  is the optimal action. For a confidence set  $\mathcal{C}$ , if for each  $P \in \mathcal{C}$ , and all the SCM that is compatible with  $P$  such that  $ATE(x) \geq 0$ , then all  $\mathcal{I}_P$  lies above zero, and therefore  $\bigcup_{P \in \mathcal{C}} \mathcal{I}_P = [\underline{L}_{ate_x}, \overline{U}_{ate_x}]$  are above zero, i.e.,  $\underline{L}_{ate_x} \geq 0$ , then the action  $x$  is better than any other actions in all SCM that compatible with all distributions in the confidence set. Therefore,  $x$  is the best action unambiguously. Similarly, if  $\overline{U}_{ate_x} < 0$ , then for all  $P \in \mathcal{C}$  and all the SCMs that are compatible with  $P$ , we have  $ATE(x) < 0$ , which indicates that in all SCMs. if  $\underline{L}_{ate_x} < 0 < \overline{U}_{ate_x}$ , by theorem 6, for all  $P \in \mathcal{C}$ , the  $\mathcal{I}_P$  contains both positive and negative value, there exist two SCM  $S_1$  and  $S_2$  such that  $x$  is the best action in  $S_1$ , but not the best action in  $S_2$ . Since this is true for all distributions in the confidence set  $\mathcal{C}$ , the best action remains ambiguous with more data.  $\square$

## E Experiments

### E.1 Causal graphs

The following causal graphs are used in our experiments.

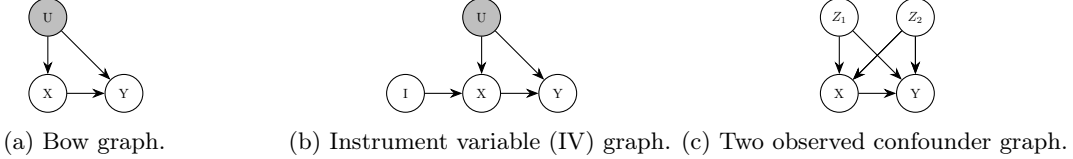


Figure 5: Causal graphs used in experiments

### E.2 Experiment detail for section 6.1

**Setup:** In the first experiments, we consider the causal graph shown in Figure 5a where we have 2 instrument variables ( $I_1, I_2$ ), one unobserved confounder ( $U$ ), a treatment ( $X$ ) and an outcome variable ( $Y$ ). All of them are considered binary. The ground truth ATE of this causal model is 0.236, i.e.,  $X_1$  is the best action. To illustrate the gradual progression of our algorithm we consider four setups: setup 1) observed variables:  $\{X, Y\}$  are sampled from  $P(x, y)$  as dataset  $D[X, Y]$  of size=1000; setup 2) observed:  $\{I_1, X, Y\}$ , are sampled from  $P(i, x, y)$  as dataset  $D[I_1, X, Y]$  of size 1000; setup 3) observed  $\{I_1, I_2, X, Y\}$  are sampled from  $P(\mathbf{V})$  as  $D[\mathbf{V}]$  of size 1000; setup 4: same as setup 3 but with 3000 samples. The goal is to choose one of the two actions  $do(X = 0)$  and  $do(X = 1)$  as the best action.

**Baselines:** Given the dataset, we estimate the corresponding joint distribution and use closed-form expression such as Tian and Pearl bound (Tian and Pearl, 2000) for bow graph with no instruments and IV bound when we have one or more instrument variables. We also use NCM (Xia et al., 2021) and autobound (Duarte et al., 2024) to obtain bounds for the input distribution.

### E.3 Experiment detail for section 6.2

**Setup:** In this experiment, we consider the causal graph shown in Figure 5c where we have 2 observed confounders ( $Z_1, Z_2$ ), a treatment ( $X$ ) and an outcome variable ( $Y$ ). All of them are considered binary. In this setup, we do not have any unobserved confounder and thus no uncertainty from non-identifiability of ATE or  $P(Y|do(X))$ . The ground truth ATE=0.06. Here we consider two setups with the same graph: setup 1) observed variables:  $\{Z_1, Z_2, X, Y\}$  are sampled from  $P(\mathbf{V})$  as dataset  $D[Z_1, Z_2, X, Y]$  of size=1000; setup 2) same as setup 1 but with 3000 samples. The goal is to choose one of the two actions  $do(X = 0)$  and  $do(X = 1)$  as the best action.

**Baselines:** Since there exists no unobserved confounders, we can compare our algorithm output with existing baselines that assume unconfoundedness. We use the dowhy package (Sharma and Kiciman, 2020; Blöbaum et al., 2024) to execute 6 baselines such as: propensity score matching, doubly robust estimator etc., on our data. These methods provides a point-wise estimation. We also execute the NCM approach which provides a bound for the ATE estimation.

### E.4 Algorithm Details

**Hyper parameters:**  $(\alpha)$ : In Alg 3, determines how fast the model's implicit distribution should return to the  $\epsilon$ -ball around the empirical distribution (i.e., controls the soft constraints).  $(\epsilon_s)$ : In Alg 1, determines the size of the search space around the empirical distribution. In general, smaller  $\epsilon_s$  values provide tighter estimates but require a larger number of candidate balls within the search space.

**Computational Complexity:** When the training dataset contains small number of samples for variables with large number of states, the search space of epsilon-net is large and therefore more iterations are needed to find the min-max and max-min. In that case, the size of epsilon-net can be adjusted with a trade-off between accuracy and efficiency. As the number of samples increases, the search space of epsilon-net will become smaller and therefore more efficient when searching for min-max and max-min. Finally, when the

empirical distribution converges to the true distribution for a large dataset, and the confidence intervals shrink accordingly, our method recovers the true bounds for non-identifiable queries, similar to existing approaches. Our main contribution lies in handling the uncertainty region where we can only estimate the empirical distributions with finite samples. We can utilize and separate the sources of uncertainty to make optimal decisions or develop data collection strategies to improve the results.

We pick each distribution  $P_{\epsilon_s}$  and train two models for at least 2000 epochs to maximize and minimize the ATE respectively while keeping the model learned distribution within  $\epsilon_s$  distance of  $P_{\epsilon_s}$ . We learn  $k$  ( $\sim 200$ ) such distributions and achieve  $k$  many  $[\min, \max, ]$  bounds. We can then construct the  $[\underline{L}_{ate}, \bar{L}_{ate}, \underline{U}_{ate}, \bar{U}_{ate}]$  following Equation 2.

All experiments were conducted on computers equipped with two NVIDIA GeForce RTX 4090 GPUs (24 GB memory each). We executed the algorithm using 15-20 parallel threads. A single run requires approximately 20 minutes, and evaluating 200 distributions is completed within 6–7 hours.